HHS Public Access

Author manuscript

Adv Biosyst. Author manuscript; available in PMC 2019 July 19.

Published in final edited form as:

Adv Biosyst. 2019 February ; 3(2): . doi:10.1002/adbi.201800252.

Endothelial Cell Mechanotransduction in the Dynamic Vascular Environment

Frank W. Charbonier,
Department of Mechanical Engineering, Stanford University, Stanford, CA, 94305

Dr. Maedeh Zamani, and
Department of Cardiothoracic Surgery, Stanford University, Stanford, CA, 94305

Prof. Ngan F. Huang
Department of Cardiothoracic Surgery, Stanford University, Stanford, CA, 94305

Veterans Affairs Palo Alto Health Care System, 3801 Miranda Avenue, Palo Alto, CA, 94304

The Stanford Cardiovascular Institute, Stanford University, Stanford, CA, 94305

Stanford University, 300 Pasteur Drive, MC 5407, Stanford, CA 94305-5407, USA

Ngan F. Huang: ngantina@stanford.edu

Abstract

The vascular endothelial cells (ECs) that line the inner layer of blood vessels are responsible for maintaining vascular homeostasis under physiological conditions. In the presence of disease or injury, ECs can become dysfunctional and contribute to a progressive decline in vascular health. ECs are constantly exposed to a variety of dynamic mechanical stimuli, including hemodynamic shear stress, pulsatile stretch, and passive signaling cues derived from the extracellular matrix. This review describes the molecular mechanisms by which ECs perceive and interpret these mechanical signals. The translational applications of mechanosensing are then discussed in the context of endothelial-to-mesenchymal transition and engineering of vascular grafts.

Table of Contents:

Physical forces provide crucial signals to the endothelial cells lining blood vessels. These instructional cues include fluid shear stress and cyclic stretch due to blood flow, as well as passive mechanical properties such as vessel stiffness and structure. Understanding how mechanical stimuli are interpreted by endothelial cells provides important insight into normal vascular function and disease progression.

Graphical Abstract

Conflict of Interest
The authors declare no conflicts of interest.

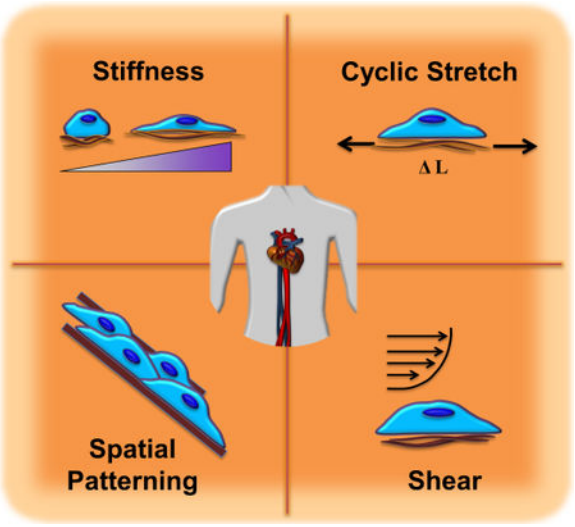

Keywords

endothelial cell; mechanotransduction; shear; endothelial-to-mesenchymal-transition; vascular graft

1. Introduction

Physical forces are integral to the physiology of all body organs. In the vascular system, blood flow imposes two types of active mechanical stimuli on the vessel wall: shear stress along the direction of blood flow and circumferential stretch caused by the pulsatile nature of blood pressure. The underlying extracellular matrix (ECM) provides additional passive cues for vascular cells, including stiffness and spatial patterning. Cells translate the perceived mechanical stimuli to biochemical signals that modulate gene expression, protein synthesis, cell proliferation, differentiation and migration. Cellular responses to physical forces in healthy blood vessels play an essential role in vascular homeostasis. Any dysregulation in the integration of mechanical stimuli can modulate endothelial permeability, inflammatory signaling, and vascular remodeling, resulting in pathological conditions associated with vascular diseases such as atherosclerosis.[1]

Blood vessels are composed of three different layers: 1) The tunica adventitia is the outermost layer of a vessel consisting of fibroblasts, collagen fibers and connective tissue; 2) The tunica media is the thick, intermediate layer comprised of smooth muscle cells, elastic fibers and connective tissue; and 3) The tunica intima is the innermost single cell layer of vascular endothelial cells (ECs) supported by a thin sub-endothelial lamina. ECs lining the innermost layer of vessel walls are in direct contact with blood flow and play crucial roles in responding to both active and passive mechanical stimuli. ECs have evolved a sophisticated mechanotransduction capability through which physical forces are translated to biochemical cues, regulating vascular function. Various endothelial-specific and non-specific upstream pathways governing mechanosensing in the vascular system have been uncovered.[1,2]

It is of great importance to identify the regulatory roles of mechanotransduction for maintaining homeostasis in healthy vascular environments and the molecular mechanisms through which ECs sense and respond to mechanical perturbations involved in vascular diseases. This knowledge provides the basis for protective approaches to prevent pathological mechanosignaling in the cardiovascular system. The integration of biomimetic mechanical signaling cues may also contribute to the development of successful tissue-engineered vascular grafts using dynamic cell culture systems and scaffolds with biologically-relevant stiffness and topography.

This review describes the major mechanical stimuli that are relevant to vascular ECs, and the molecular mechanisms by which ECs perceive and interpret these signals. The translational applications of mechanosensing in endothelial-to-mesenchymal transition and engineering of vascular grafts are also presented.

2. Mechanisms of Cellular Mechanotransduction

2.1 Ion Channels, Endothelial Glycocalyx, and the Cell Membrane

Mechanical stimuli are transduced to biochemical signals, often by conformational protein changes. For example, mechanical strain stimulates stretch-activated (SA) ion channels through changes in membrane tension or curvature. These channels allow for the passive flow of ions though the membrane and may be mechanically gated, with reversible open or closed states. In-plane stretch increases or decreases the probability of each state, thus regulating the flux of ions such as Ca^{2+}. Intracellular calcium signaling is ubiquitous and capable of generating rapid downstream responses.[3] Piezo1 and Transient Receptor Potential (TRP) Cation Channel Subfamily V Member 4 (TRPV4) are mechanosensitive ion channels that play a role in flow sensing and downstream regulation of vascular tone by constriction or dilation of blood vessels.[4,5] Piezo1 also appears to be essential for shear-mediated vascular development.[6]

The endothelial glycocalyx is a bush-like network that separates the cell membrane from the fluid above and participates in hemodynamic flow sensing. This carbohydrate-rich mesh consists of proteoglycans, glycoproteins, and glycosaminoglycans (GAGs), the most important of which are heparan sulfate, chondroitin sulfate, and hyaluronan.[7] A periodic arrangement of core proteins may dampen shear stresses felt at the membrane surface, but also transmit and amplify tip forces to the mechanically-coupled cytoskeleton and trigger signaling cascades.[8] One example of mechanosensing by the glycocalyx is the stimulation of nitric oxide (NO) production in a TRP channel-dependent manner in response to shear.[9] Secondary messengers such as NO, can rapidly diffuse within and throughout the cell to produce global responses. NO promotes vasodilation and reduced expression of adhesion molecules as well as suppresses nuclear factor kappa-light-chain-enhancer of activated B cells (NFκB), a major regulator of inflammation. Meanwhile, reactive oxygen species (ROS) suppress expression of endothelial NO synthase (eNOS), stimulate monocyte adhesion, and promote EC dysfunction.[10] The balance between NO and ROS determines the state of oxidative stress and thus regulates vascular homeostasis.

Spatial and temporal changes in local or global membrane properties induce conformational changes in transmembrane proteins spanning the bilayer. Membrane fluidity alters the physical proximity of and biochemical interactions between proteins floating in the membrane such as G-protein-coupled receptors (GPCRs), which are an integral part of regulation pathways. Shear can thus directly stimulate GPCRs, which in turn activate kinases to phosphorylate proteins and set of signaling cascades.[11] Local microdomains within the membrane such as lipid rafts or caveolae may concentrate signaling molecules and enhance reaction rates.[12] Caveolae are membrane invaginations that rapidly flatten to compensate for surface area changes following cell stretching or osmotic expansion. In addition to mediating shear-induced activation of the ERK pathway, these membrane structures are potentially the primary source of passive stress compensation to prevent spikes in membrane tension.[13] Lipid rafts are regions of increased cholesterol content that modulate SA channel sensitivity by changing local membrane stiffness.[14] Patterns of oscillatory shear stress can also decrease membrane fluidity and affect membrane-bound proteins, especially those tightly packed in lipid rafts (e.g. integrin α5). Integrin activation by oscillatory flow to produce downstream disruption of the endothelium required translocation to lipid rafts. The lipid raft protein caveolin-1, along with F-actin and cholesterol, is involved in sequestration of integrin α5 into these microdomains.[15]

2.2 Cell-ECM and Cell-Cell Mechanotransduction

A variety of mechanical cues are transduced between ECs and the surrounding ECM. ECs reside in a basement membrane consisting of proteoglycans and proteins such as collagen IV, laminin, and fibronectin. [16] Adhesions between the cell and the underlying ECM provide a structural basis for mechanosensing. Integrins are key transmembrane proteins which bind to ECM ligands at specific domains (e.g. RGD) and are linked to the actin cytoskeleton indirectly though other molecules. Binding causes integrins to cluster and form focal adhesion complexes that provide physical coupling between the cell and the external mechanical environment. These activated integrins recruit talin, paxillin, FAK, α-actinin, and actin to cluster at the adhesion in the absence of force, but not vinculin. Forces applied to fibronectin-coated beads were shown to induce vinculin recruitment,[17] and it was later shown that talin stretching led to unfolding and opening of previously hidden binding sites for vinculin recruitment.[18] This molecular mechanism by which forces unravel proteins to expose cryptic binding sites and trigger enzymatic activity and intracellular signaling cascades is similar for α-actinin.[19]

Small GTPases such as RhoA, Rac1, and Cdc42, all members of the Rho family, are important signaling proteins for cell adhesion, migration, and morphology. RhoA can stimulate stress fiber formation by actin polymerization.[20] RhoA/Rho kinase (ROCK) signaling is a key mediator of many effects related to substrate mechanics, such as the feedback between focal adhesions, cell shape, vessel stiffness, and actomyosin contractility. [21,22] Rac is involved in the formation of lamellipodia and filopodia by recruitment of integrins,[23] and by vinculin signaling.[24] The spatial distribution of intracellular Rac resulting from the organization of ECM adhesions by cell shape could influence the formation of protrusions and directional migration.[25] A large assortment of additional

signaling molecules and pathways are implicated in endothelial mechanosensing and have been reviewed elsewhere.[26]

Focal adhesions rely on connection to the cytoskeleton to function as sites of active force transmission and mechanosensing. The actin cytoskeleton is a dynamic filamentous network which is heavily involved in both structural and signaling behaviors and can play an indirect role in mechanotransduction by transferring loads from peripheral adhesions to mechanosensory molecules or even directly to the nucleus. Direct deformation of a substrate will deform focal adhesions and thus the cytoskeleton. Similarly, flow can be transmitted to focal adhesions through the cytoskeleton via “outside-in” mechanosensing.[2] Another key feature of the cytoskeleton is “inside-out” sensing by the generation of forces to probe changes in external mechanical properties such as ECM stiffness. [2] Myosin motor proteins pull on actin filaments to generate tension and produce intracellular contractile forces.[27] RhoA-mediated actomyosin contraction leads to maturation of focal adhesion complexes through robust feedback loops.[28] Recent studies demonstrate that cells use contractile pinching for rigidity sensing, in which small, pulsed contractions of uniform deformation build up to and exceed a force threshold for reinforcement of adhesions.[29]

While integrin adhesions to the ECM provide coupling to the external environment, endothelial cell-cell junctions are also important regulators of both mechanosensing and permeability. Platelet endothelial cell adhesion molecule (PECAM-1/CD31) at cell junctions is activated rapidly when exposed to shear and forms a complex with vascular endothelial cadherin (VE-cadherin) and vascular endothelial growth factor receptor 2 (VEGFR2).[30] This triggers RhoA-mediated reorganization of the cytoskeleton and changes in contractility, which contribute to the global state of intracellular stresses and junction tension.[31] Forces across junctional proteins are also linked to cell-matrix adhesions, with CD31 signaling triggering integrin formation following PI3-K activation.[32]

The sequence of mechanotransduction events has been described.[33] Within the first seconds of mechanical stimulation there is immediate sensing by SA ion channels and force-dependent conformational changes (e.g. talin unfolding). Subsequent biochemical cascades are mediated by Ca^{2+} influx or G-proteins such as Rho, followed by contraction or actin polymerization on the timescale of several seconds to minutes. The emerging picture seems to be that cells are continually sensing mechanical cues and integrating signals over time to produce long term changes in behavior and fate (Figure 1).

2.3 Nuclear Mechanotransduction

Donald Ingber introduced tensegrity models of the cell and theorized in 1993 that such a structure could transmit forces almost instantaneously throughout an integrated cytoskeletal network.[34] He and others later demonstrated that forces could be transferred directly to the nucleus to distort the nuclear envelope,[35] and that this mechanical transmission could occur on timescales an order of magnitude faster than growth factor signaling.[36] A physical connection between the nucleus and cytoskeleton has since been provided by discovery of the Linker of Nucleoskeleton and Cytoskeleton (LINC) complex.[37]

The cytoskeleton can directly pull on the nucleus, which in turn responds to tension. Nuclear mechanotransduction models aim to link mechanical stimuli with gene expression and control of cellular behavior on longer timescales. Understanding the physical contributions of lamins and other structural proteins will aid in understanding these mechanosensing loops. For example, nuclear viscoelasticity is dependent on the ratio of lamin A (LMNA) and lamin B (LMNB), and LMNA interacts with chromatin.[38] Nuclear membrane complex-associated transcription factors may bind to and transcribe exposed regions of the genome. One pair of transcription factors linked with mechanotransduction is Yes-associated protein (YAP) and transcriptional coactivator with PDZ-binding motif (TAZ). YAP/TAZ plays a key role in RhoA/actomyosin dependent mechanotransduction of substrate stiffness and cell shape.[39] Inactive phosphorylated YAP/TAZ remains localized in the cytoplasm, whereas activated YAP/TAZ translocates to the nucleus and promotes upregulation of target genes. Activated YAP/TAZ has been shown to mediate the inflammatory response of ECs to oscillatory shear, with high proliferation and turnover in oscillatory shear and cell cycle suppression under laminar shear.[40] YAP/TAZ may also be regulated by VE-cadherin/PI3K,[41] integrins,[42] and GPCR signaling.[43]

Epigenetic regulation is increasing noted for its important role in flow-regulated vascular function.[44] MicroRNAs,[45–47] histone deacetylases,[48] and DNA methyltransferases (DNMTs) provide mechanosensitive control of gene expression to produce heritable phenotypic heterogeneities in endothelial cells. DNA methylation is one such epigenetic mechanism for silencing of genes and plays important role in normal vascular physiological function and disease pathology.[49] DMNTs are responsible for adding methyl groups to DNA to repress transcription.[50] Shear stress affects expression nuclear localization of DMNT1 to differentially regulate DNA methylation *in vitro* and *in vivo* under oscillatory and laminar flow conditions.[49]

3. Mechanical Stimuli in the Vasculature

ECs in living organisms exist in a highly dynamic mechanical environment. Blood flow through the vasculature supplies hemodynamic forces along with biochemical factors, while vessel architecture and composition provide stiffness and spatial cues. The mechanosensitive endothelium integrates these diverse stimuli through cell-matrix adhesions, cell-cell junctions, and intricate yet robust transduction mechanisms. Thus, physical forces play a key role in normal EC function as well as the pathology of vascular diseases such as atherosclerosis.

3.1 Shear stress

Hydrodynamic stresses from blood flow provide key mechanical stimuli for vascular adaptation and homeostatic function. The endothelium is subjected to shear stresses of 0.1–0.6 Pa (1–6 dynes • cm^{-2}) in veins and 1–7 Pa (10–70 dynes • cm^{-2}) in arteries.[51] Blood flow is highly pulsatile in arteries and less pulsatile in veins.[52] Unidirectional laminar flow in blood vessels with orderly fluid streamlines producing wall shear stresses of ~1.2 Pa is considered protective against the accumulation of lipids that contribute to atherosclerosis. Conversely, complex patterns of disturbed flow in which fluctuating shear stresses can drop

to 0 Pa and exhibit disordered changes of direction have been implicated in endothelial dysfunction. Complex disturbed flow often occurs in curved or branched vessel regions, such as arterial bifurcations and the aortic arch.[53] The increased endothelial permeability to lipid uptake can make these sites susceptible to the formation of atherosclerotic plaques.[54,55]

Flow-induced shear stress has traditionally been recognized as a key mechanical stimulus directing EC behavior. Bovine aortic ECs (BAECs) reorganize and align along the direction of shear flow, orienting their cytoskeleton accordingly and elongating parallel to the flow direction.[56,57] BAECs subjected to 1.52 Pa shear stress first reinforced substrate adhesions as indicated by vinculin staining and increased the number of F-actin stress fibers in order to remain attached. After 6 hours, cells overcame the restrictions of cell-cell adhesions and reoriented in line with the flow direction. Eventually the BAECs elongated along the flow direction and strengthened cell-substrate and cell-cell adhesions to reinforce the tight monolayer. The resulting ellipsoidal shape and spatial rearrangement of cells appeared to minimize intracellular stresses.[58]

The endothelial response to hemodynamic forces varies with flow regimes. Sustained and uniform laminar flow confers protective benefits from atherosclerosis by maintaining non-proliferative and anti-inflammatory gene expression profiles. Laminar shear stimulates production of NO and expression of eNOS, while irregular patterns of disturbed flow inhibit NO production and contribute to oxidative stress.[10]. Sustained inflammatory and proliferative signals during disturbed flow lead to higher EC turnover and increased monolayer permeability, which are key events in atherogenesis.[59] Confluent BAEC monolayers were sensitive to turbulent flow at wall shear stresses as low as 0.15 Pa, while 0.8 Pa was required for laminar flow reorganization. EC turnover increased under turbulent flow as compared to static or laminar conditions, with significant cell rounding and increases in DNA synthesis by 16 hours of flow exposure preceding gap formation in the monolayer at 24 hours (Figure 2).[60] Confluent human umbilical vein EC (HUVEC) monolayers subjected to varying flow regions in a step channel were more elongated in regions of higher stress. Well-organized cytoskeletons with thick, aligned actin stress fibers were observed in fully developed laminar flow regions, while cells experiencing stress fluctuations and high shear gradients in disturbed flow regions displayed increased cell rounding and DNA synthesis.[61]

Active cytoskeletal reorganization is closely linked to both cell-substrate and cell-cell adhesions. VE-cadherin is an adhesive protein which plays an important role in maintaining EC junctional integrity and regulating endothelial permeability. Flow patterns and the resulting wall shear characteristics can modulate the distribution of such proteins along cell-cell junctions. VE-cadherin staining at EC borders was stronger in long, straight regions of a rat thoracic aorta where laminar flow dominated, while it was weaker in regions of disturbed flow such as the aortic arch and downstream of an induced vessel constriction. These *in vivo* observations were supported by findings following exposure of confluent BAEC monolayers to pulsatile flow (1.2 ± 0.4 Pa) and oscillatory flow (0.05 ± 0.4 Pa) *in vitro*. After six hours, the ECs in both flow groups displayed intermittent staining of VE-cadherin, while static control samples showed continuous VE-cadherin staining along the cell borders. Beyond 24

hours, pulsatile flow conditions led to recovery of continuous and uniform VE-cadherin staining, whereas ECs under oscillatory conditions continued to display intermittent gaps in staining. Interestingly, immunoblots revealed that the flow conditions affected neither protein expression levels nor the membrane-cytosol fraction of VE-cadherin, suggesting that VE-cadherin redistribution was modulated by the temporal characteristics of shear stress and was responsible for the observed differences in junctional integrity.[62]

VE-cadherin, along with VEGFR2 and CD31, form a key mechanosensory complex at EC junctions responsible for flow sensing. Blocking any of the components of this complex eliminated the morphological responses of cytoskeletal rearrangement, elongation, and alignment with flow.[30] Interestingly, tension across VE-cadherin decreases upon shear whereas it increases across CD31.[63] This was suggested to be evidence of an active rather than passive cytoskeletal response, in which flow sensing by a different mechanosensory component triggers vimentin cytoskeleton association with CD31 to bear tension from myosin across cell-cell junctions and form the mechanosensory complex with VE-cadherin and VEGFR2.[52] Tension on CD31 sets off a cascade of signaling in response to flow, which first requires that the transmembrane domain of VE-cadherin functions as an adaptor and binds to the transmembrane domains of VEGFR2 and VEGFR3. This event then triggers P13K activation, production of NO, and vasodilation. PI3K also activates integrin binding to align cells in the direction of flow.[52]

Hydrodynamic drag on the nucleus may provide an upstream mechanism of EC flow sensing. It was shown that confluent HUVEC monolayers exposed to shear stress of 0.72 Pa or greater became gradually polarized against the flow, in which the nucleus was pushed downstream relative to the microtubule organizing center (MTOC) or Golgi apparatus. For ECs on the upstream side of a monolayer scratch wound, cytoskeletal reorganization produced a dense lamellar mesh of actin that prevented nuclear displacement and produced polarization along rather than against the direction of flow. Although confluent ECs displayed cortical actin bundles localized to cell-cell junctions, these bundles disappeared upon wounding and were replaced by lamella and lamellipodia. The opposing polarity in each of the two conditions highlighted the importance of cell-cell contacts and cytoskeletal organization in flow sensing. In confirmation of this prediction, destabilization of the actin cytoskeleton by latrunculin or myosin-II inhibition enhanced downstream nuclear displacement and polarization against flow in non-confluent ECs. Furthermore, application of a large hydrodynamic force for less than 5 seconds pushed EC nuclei an average of 8μm downstream and induced polarization that persisted for over an hour in the absence of flow. This model for EC flow sensing suggests that the cytoskeleton resists nuclear drag and thus modulates the sensitivity of polarization to wall shear.[64] Together, these studies demonstrate the strong influence of shear stress in the modulation of EC function and behavior.

3.2 Topography and Spatial Patterning

Given the hierarchically organized architecture of the native vascular environment, topography and spatial arrangement of the ECM might provide instructional cues to guide EC behavior and fate. Increased spreading of bovine capillary ECs on square, fibronectin-

coated islands from 75 to 3000 μm^2 correlated with increased DNA synthesis and decreased apoptosis. This trend of enhanced growth and reduced cell death with increasing cell spreading area continued for ECs spread across arrays of small, closely-spaced circular islands which equalized the total ligand contact area.[65]

Follow-up studies of bovine capillary ECs confined to 10 and 30 μm-width lines displayed a similar relationship between increased spreading area and the balance of cell growth and death. ECs were most spread (projected area = 3112 μm^2) on unpatterned surfaces as compared to 30 μm lines (2200 μm^2) and 10 μm lines (1042 μm^2), with only one or two cells extending across the pattern width for 10 μm columns. The most highly spread cells proliferated nearly twice as fast as the least spread cells in the first 24 hours. By 72 hours, proliferation stopped altogether on the 10μm patterns and ECs formed multicellular capillary tubes with a hollow lumen aligned along the linear pattern. Continuous staining of CD31 along the lumen indicated a complete junctional seal and fibronectin remodeling produced a single organized tendril aligned beneath the tube. ECs also elongated and aligned their cytoskeletons along the 30μm linear patterns and stained for CD31 along cell-cell junctions, but they did not form lumens or coalesce the remodeled extracellular fibronectin fibrils.[66]

Similar micropatterned strips of collagen were used to demonstrate the role of geometric cues in migratory behavior of ECs. BAECs on narrow (15μm) patterns were more elongated (cell shape index ~0.3), less spread, and more oriented in the direction of the pattern than on 30μm and 60μm patterns. Subsequently, BAECs displayed more persistent directional migration and significantly higher migration speeds on thinner patterns. The migration velocity component V_x along the axis of linear patterns was higher than the orthogonal component V_y for all line widths, but a significantly larger (~4-fold) difference was observed for the 15μm strips.[67] The direction of EC migration may be influenced by the distribution of traction forces exerted by the cell on the ECM. When cultured on square patterns, bovine capillary ECs developed diagonally-oriented stress fibers as visualized by phalloidin staining of actin filaments. These cells preferentially extended F-actin containing lamellipodia and filopodia from the corners of the patterns, where tractional stresses were highest, whereas cells on round patterns extended randomly distributed protrusions. These protrusions disappeared upon disruption with myosin or ROCK inhibitors.[68]

ECs are also capable of sensing topographical cues and gradients therein. BAECs on elastomeric substrates with rounded 0.45 μm deep grooves showed increasing alignment with the pattern and elongation with decreasing periodicity of the parallel ridges and grooves from 4.5 to 2.5 μm.[69] Alignment and elongation of rat aortic ECs increased significantly as pattern dimensions of a periodic array of titanium grooves decreased from 100 μm to 750 nm. Additionally, ECs required less time to reach confluency as the topographical length scale of surface patterning decreased.[70] Endothelial progenitor cells (EPCs) on nanotopographically patterned surfaces with 600 nm-wide grooves and ridges were aligned and elongated, and exhibited reduced proliferation and enhanced directional migration velocity as compared to EPCs on flat substrates. Furthermore, while cells on flat substrates eventually formed confluent monolayers, those on patterned surfaces formed distinct band-like multicellular structures with alignment and organization that persisted over long term six-day culture. Upon addition of Matrigel, EPCs on the nanopatterned surfaces displayed

higher frequency and efficiency of capillary tube formation, with longer and more organized tubes.[71] Aligned collagen was used to generate anisotropic nanoscale topography without requiring cellular confinement within micro-grooves. Primary human dermal microvascular ECs showed greater cellular alignment and organization of focal adhesions as visualized by paxillin staining, with focal adhesions clustered at the front and back of cells on anisotropic nanofibers vs uniformly distributed throughout for randomly oriented collagen. Timelapse microscopy also revealed preferential orientation of protrusions and quicker migration along the fibril direction.[72]

Several studies have explored the effects of combining multiple, distinct mechanical stimuli. HUVECs on electrospun fibers were exposed to simultaneous chemical gradients of vascular endothelial growth factor (VEGF). Whereas persistent directional migration was maximized when the chemical gradient was parallel to the fiber direction, the chemotactic effect was abrogated when fibers were oriented perpendicular to the VEGF gradient. This suggested that topography could dominate over biochemical cues in directing cellular migration.[73] Similarly, nanotopographical cues dominated over flow direction for primary human dermal ECs exposed to spatially varying shear flow. ECs adopted and retained an elongated morphology and migrated along the direction of aligned nanofibrillar collagen films even in regions where shear stress was applied orthogonal to the fibril alignment. Furthermore, the aligned spatial patterning produced significant reductions in pro-inflammatory function as quantified by monocyte adhesion and intercellular adhesion molecule 1 (ICAM-1) expression, as well as reduced EC turnover. CD31 junctional thickness and continuity were similarly enhanced by topographical alignment (Figure 3).[74] Given the influence of cell shape in directing endothelial growth, death, morphogenesis, and function, spatial patterning warrants further study. The limited present understanding of topographical cues has already seen direct translation to tissue engineering applications, which will be covered in a later section.

3.3 Extracellular Matrix Stiffness

Substrate stiffness plays a major role in cellular behavior across a range of cell types and has been reviewed extensively elsewhere.[75] The rigidity of substrates underlying or encapsulating cells can directly instruct morphology, function, and even differentiation.[76] Stiffness can produce varied effects between cell types.[77] Here, we will focus on the effects of stiffness on ECs (Table 1).

The endothelium in blood vessels sits on a thin intimal basement membrane surrounded by thick medial and adventitial layers providing strength and elasticity. Measurements of vascular stiffness are complicated by the inclusion or exclusion of these varying structural components and by non-uniform testing methods. As a result, the reported range of ECM stiffnesses relevant for ECs can vary greatly. Pressure-strain relationships give an indication of the bulk properties of a vessel but are dependent on the global geometry. Local material properties may be more accurately assessed by methods such as atomic force microscopy (AFM), in which a small cantilever tip is used to indent the specimen and the resulting deflection is tracked to calculate the elastic modulus.

Porcine carotid artery stiffness was 5 to 8 kPA as measured by AFM indentation on the medial layer, which consists of primarily smooth muscle tissue.[78] Additional AFM measurements of elastic modulus have produced values of 3.2 kPa for murine femoral artery and 4.3 kPa for the murine thoracic aorta for mice,[79] and ~2.5 kPa for the subendothelial layer in bovine carotid arteries after scraping.[80] The relative size and proximity of the various layers may make bovine samples the best analog for human vessels.[81] The stiffness of blood vessels also increases with age and injury.[82,83] Pathological stiffening has been reported to exceed 100 kPa in the calcified lesions of atherosclerotic rabbit thoracic arteries as measured by local pipette aspiration.[83]

Meanwhile, the stiffness of standard tissue culture polystyrene(~3 GPa) and glass (~50 GPa) are markedly higher and greatly exceed that of any tissue in the body.[84]

Engineered substrates that mimic a more physiologically relevant range of matrix rigidity show clear morphological effects on ECs *in vitro*. BAECs sparsely cultured on soft 0.18 kPa gels were rounded whereas on stiffer (2.9 kPa and 28.6 kPa) gels they were more spread and spindle-like. However, these morphological differences disappeared once cell-cell contacts were established and ECs on both soft and stiff gels were able to divide and form visually identical confluent monolayers.[77] The proliferation of HUVECs on polyacrylamide (PA) gels increased with increasing gel stiffness from 1.72 kPa to 21.5 kPa, and matrix rigidity regulated the activity of cell cycle-associated proteins. As with prior studies, cells on stiffer gels were more spindle-like and spread with higher F-actin staining than the smaller, rounded cells on the more compliant substrate. ECs on softer gels had higher concentrations of actin at the peripheral cortical layer as compared with ECs on stiffer gels. Softer gels led to lower RhoA activity compared to stiffer gels, with stiffer gels promoting activation of $\alpha 5\beta 3$ integrins, increased formation and distribution of actin stress fibers, and enhanced proliferation. The addition of constitutively active RhoA to ECs on softer gels lead to increased stress fiber formation and a corresponding increase in the number of ECs entering the cell cycle.[85]

A study of primary porcine ECs on PA gels suggested that a balance of EC contractility and cell-cell junction integrity may be necessary for directed collective migration. ECs migrated farthest on the most rigid 50 kPa gels but had the highest nuclear alignment in the migration direction on 14 kPa intermediate stiffness gels and the highest junction integrity on the softest 4 kPa gels. Elevation of cytoskeletal tension above a certain threshold by actomyosin contractility may overcome the junction's ability to remain intact. Depletion of contractility by ROCK inhibition did not affect the migration distance significantly on stiff gels but did increase migration distance on 4 and 14 kPa gels. ROCK inhibition also equalized the fraction of cells aligned in the migration direction for all conditions by increasing alignment on stiffer gels. ECs remodel the ECM as they align during collective migration, and this study observed that EC-deposited fibronectin fibers were more aligned in the migration direction on stiffer gels. Finally, knockdown of the $\alpha 5\beta 1$ integrin reduced migration for ECs on 14 and 50 kPa gels and eliminated differences in migration distance between the 3 stiffness conditions tested.[86]

BAECs cultured for 4 hours on 2.5 kPa PA gels with covalently bound RGD ligand at varying ligand densities showed quicker and more isotropic spreading on surfaces with higher ligand density and contraction, which was linearly correlated with cell spreading area. Furthermore, significant cellular traction forces could be generated within minutes of plating and before the formation of actin stress fibers and vinculin-containing focal adhesions. Stress fiber formation and focal adhesions appeared within one hour and F-actin peaked at three hours.[87] A follow-up study found that spreading area and stiffness were key predictors of force generation in BAECs and suggested that cell-cell adhesions and cytoskeletal reorganization preceded an increase in contractility. Traction forces elevated when cells came into contact and the relative increase was greater on higher stiffness.[88]

Stiffness plays a key role in endothelium integrity, which is of great pathological importance in atherosclerosis. Traction force microscopy (TFM) of HUVEC monolayers patterned on 1.2 kPa to 90 kPa PA gels revealed that cells were more contractile on stiffer gels. Adding thrombin to induce hyperpermeability enhanced traction forces on both soft and stiff gels. For soft gels, this increase was primarily located at the monolayer edges and resulted in increased staining of diffuse F-actin, whereas on more rigid gels the traction force hot spots were distributed throughout the monolayer. On stiff gels, the addition of thrombin resulted in formation of distinct actin stress fibers and large gaps in the monolayer at the locations of greatest traction force. When a VE-cadherin blocking antibody was incubated with the cells to break cell-cell junctions, it was shown that VE-cadherin sustained higher forces on stiffer substrates and represented roughly half of the overall monolayer forces in all conditions. The addition of thrombin resulted in significant enhancement of ROCK activity on all substrates, with the greatest enhancement appearing for the most rigid gels. ROCK inhibition with Y-27632 reduced overall baseline forces and protected monolayers from gap formation even with thrombin stimulation on the stiffer 11 kPa substrates.[89] Similar *in vitro* results showed increased permeability of BAEC monolayers to dextran dye as stiffness of PA gels increased from 3.5 to 10 kPa. These findings were validated with a mouse model of aging. The relative subendothelial stiffness of thoracic aortas increased significantly between 10 and 25 months and corresponded to greater dye permeability as well as greater VE-cadherin junction width with age.[81]

The balance of inter- and intra-cellular forces by Rho-mediated contraction appears to play a key role in regulating the response of endothelial monolayers to stiffness and changes in barrier function. Multiple mechanical stimuli can be integrated by a global cytoskeletal network, and loading at specific locations not only triggers local changes but can lead to junctional remodeling in distant cells.[31] Magnetic twisting cytometry was used to activate VE-cadherin mechanosensing for human pulmonary aortic ECs on 1.1 kPa and 40 kPa PA gels or glass substrates. Two minutes of loading triggered increases in cell stiffness and VE-cadherin gap formation, with greater increases in cell stiffness on softer gels and significantly larger increases in gap area on the stiffer substrates. Bead twisting also resulted in significant increases in paxillin-stained focal adhesion number and size on stiffer substrates but not on the softer gel, potentially indicative of inside-out signaling. TFM and MSM (monolayer stress microscopy) revealed that increasing matrix rigidity raised the average EC monolayer stress as well as enhanced fluctuations in monolayer stress, thus increasing susceptibility to gap formation.[53] Accordingly, Stroka and Aranda-Espinoza

found that the fraction of neutrophils transmigrating across tumor necrosis factor-α (TNF-α)-stimulated HUVEC monolayers increased with increasing stiffness (0.42 to 280 kPa) of PA gels. This increased transmigration produced large holes in the monolayer on more rigid substrates and was not the result of changes in ICAM-1 expression, which remained constant with changing rigidity. Disrupting cell-cell junctions with a VE-cadherin antibody reduced the number of transmigrating neutrophils but only on soft 0.87 kPa substrates, while blocking contraction with a myosin light chain kinase inhibitor reduced transmigration on stiffer (5 kPa and 280 kPa) substrates almost to the level of the soft gels.[90]

Motivated by findings that intima stiffness heterogeneity can increase with age,[91] Burdick and colleagues cultured BAECs on photopatterned hyaluronic acid-based hydrogels with a checkerboard array of 2.2 kPa and 10.3 kPa squares. Larger and more mature vinculin-stained focal adhesions were produced on stiffer matrix regions, and increased spatial stiffness heterogeneity disrupted junctional integrity of confluent endothelial monolayers as visualized by the size and frequency of intercellular gaps in VE-cadherin staining.[92]

Researchers have also studied the influence of hydrodynamic forces on stiffness sensing. Sub-confluent BAECs exposed to flow for 24 hours aligned at lower levels of shear on more rigid substrates. Substantial alignment was observed at 0.6 Pa shear on 10 kPa gels, while 2.2 Pa shear was required to achieve similar alignment on 100 Pa substrates. The impact of flow on spreading area was reduced for cells on 10 kPa substrates, but there was a significant increase in spreading on 100 Pa gels at shear stress above 1.2 Pa. AFM measurements of cell stiffness increased for all experimental groups with flow as compared to static controls, though this change was more rapid and of larger magnitude for decreasing matrix rigidity. Finally, disruption of the glycocalyx component hyaluronan by blocking synthesis or degrading existing hyaluronan for cells on soft 100 Pa gels did not affect spreading under static conditions but blocked spreading at all applied levels of shear, up to 2.2 Pa.[93]

Substrate stiffness plays a key role in endothelial cell migration, turnover, junctional integrity, and vascular morphogenesis. Traction forces are both produced and balanced by the actomyosin cytoskeleton to regulate the effects of matrix rigidity. This understanding has far-reaching and direct implications in research. As an example, many studies are still done on rigid surfaces, which may markedly affect cytoskeletal organization, force generation, and signaling as compared to substrates of physiological stiffness.

3.4 Cyclic Stretch

ECs *in vivo* are subjected to cyclical stretch as blood vessels expand and contract. A strain of 5 to 10% is considered normal for arteries, while levels greater than 20% such as those seen in hypertension are considered pathological.[94] Stretch has been implicated in vessel adaptation in the form of matrix metalloproteinase (MMP) remodeling by as well as vasodilation.[95,96]. Physiological levels of stretch are believed to maintain vasculature health by regulating endothelial morphology, migration, proliferation, inflammation, and angiogenesis. Many of these effects have been reviewed in depth elsewhere.[97]

ECs on unpatterned surfaces appear to align perpendicular to the direction of applied stretch, with the development of stress fibers playing a key role.[98] Complex strain fields can make

it difficult to distinguish the contributions of elongation and compression to endothelial morphology. Pulling a substrate in one direction will contract it in the orthogonal direction and complicate the evaluation of causation. Subjecting sparsely seeded human aortic ECs to 3 different stretch conditions enabled direct comparisons. Compression is highest at 90 degrees from the primary stretch direction for simple unconstrained elongation, while no deformation is allowed perpendicular to the stretch axis in the uniaxial configuration. ECs oriented perpendicular to the direction of cyclic 10% uniaxial stretch within 3 hours and could re-orient along a new axis when the stretch direction was rotated 90 degrees. ECs specifically aligned along the direction of minimal substrate deformation, which was 70 degrees from the stretch direction for simple elongation and 90 degrees for uniaxial stretch. Meanwhile, equal biaxial stress resulted in tent-like protrusions out of the stretch plane. Additionally, the magnitude of stretch dominated over stretch rate at early time points under 2 hours.[99]

Cell turnover plays an important role in atherosclerosis and may also be subject to regulation by stretch. BAECs were subjected to cyclical strain at 1 Hz and changes in cell viability, DNA laddering, and caspase-3 activity were tracked. While physiologically normal levels of 6% and 10% stretch negated the cytotoxic effects of TNF-α, 20% strain increased TNF-α-mediated apoptosis. 6% strain activated Akt, which is downstream of PI3k, and PI3k inhibitors reversed the protective effects.[100]

HUVECs subjected to 20% strain at 1 Hz displayed up to 3-fold and 3.7-fold higher mRNA expression and protein levels at 18 hours of MMP-2 and MMP-14, respectively. Meanwhile, MMP levels for ECs with 10% stretch at 1 Hz were unchanged from unstretched controls. Cyclic 20% stretch increased TNF-α production beginning from 2 hours following initiation of stretch and reaching a maximum at 12 hours. The effects of stretch on MMP activity were abrogated by addition of a TNF-α blocking antibody.[95]

The early influences of cyclic strain (7 and 24%) at 1 Hz on focal adhesion proteins have been explored. The phosphorylation of focal adhesion kinase and vinculin increased within 30 minutes and 4 hours, respectively, and mirrored the spatial rearrangement of these proteins along F-actin filaments. Inhibiting phosphorylation with tyrphostin blocked these strain-induced increases as well as the morphological alignment of cells perpendicular to stretch.[101] TRPV4 was shown to be at least one of the SA ion channels responsible for this reorganization. Static stretch of 15% applied to bovine capillary ECs triggered calcium influx within 5 seconds, and SA-channel activation was necessary for downstream activation of PI3K within 1 minute of static stretch and activation of α5β1 integrins to stimulate further fibronectin binding. This sequence was necessary for the reorganization of ECs in response to cyclical stretch for both bovine and human CEs.[102]

Blood flow produces shear stress and cyclic vessel stretch which, along with topography and stiffness, combine to regulate endothelial cell structure, behavior, and function in vascular homeostasis and disease. Through a continual process of mechanosensing, ECs actively integrate these active and passive physical cues into specific cellular responses (Table 2). In the following sections we will discuss how this mechanotransduction machinery contributes

to regulatory and pathological phenomena, as well as how our understanding may translate to improved clinical outcomes in medical applications.

4. Applications of Vascular Mechanobiology

4.1 Endothelial-to-mesenchymal transition

Endothelial-to-mesenchymal transition (EndMT) is the process by which ECs undergo changes in gene expression, morphology, and behavior to acquire a multipotent mesenchymal-like state.[103] As in the related process of epithelial to mesenchymal transition (EMT), these cells disassemble cell-cell adhesions and alter morphology to become more migratory and spindle-like. During EndMT cells lose typical EC markers such as VE-cadherin, CD31, and von Willebrand factor (vWF). They begin to express mesenchymal markers such as fibroblast-specific protein-1 (FSP-1), alpha-smooth muscle actin (α−SMA), and vimentin,[104] and may transdifferentiate into smooth muscle cells, fibroblasts, and even osteoprogenitors.[103] Accompanying the transition to a mesenchymal-like phenotype is an increase in MMP activity (e.g. MMP-2 and MMP-9) which degrades the basal lamina. Furthermore, EndMT-derived cells may secrete more collagen I and III and fibronectin, with upregulation of stiffer ECM proteins and remodeling leading to loss of elasticity and fibrosis (Figure 4).[104]

EndMT plays an important role in cardiovascular formation during normal embryonic development.[105] However, it is also implicated in a wide range of fibrosis-related pathologies including vascular disease,[106] and as source of cancer associated fibroblasts.[107,108] Recently, the contribution of endothelial-derived fibroblast-like cells to intimal atherosclerotic plaques was demonstrated by lineage tracing in mice. EndMT produced a population of cells distinct from both normal endothelial cells and fibroblasts which showed increased expression and release of MMPs, a trademark of atherosclerotic plaque instability, but less collagen gene expression as compared to fibroblasts. The number of transitioning EndMT-derived fibroblast-like cells correlated with increased likelihood of rupture in complex human plaques.[109] Similar lineage tracing techniques uncovered roles in cardiac fibrosis for transforming growth factor beta (TGF-β)-mediated EndMT.[110]

TGF-β is a pleiotropic secreted cytokine widely recognized as a major regulator of EndMT. TGF-β signaling through activation of the ALK1 receptor inhibits EndMT, but TGF-β signaling through ALK5 promotes EndMT by activating Smad2/Smad3, which form a complex with Smad4 that interacts with the EndMT-associated transcription factors Snail, Slug, and Twist in the nucleus.[107] These transcription factors contribute to the expression of mesenchymal target genes. Rho activation by TGF-β can assist in the expression of EndMT-related transcription factors,[111] while fibroblast growth factor (FGF) signaling through the adaptor molecule FGF receptor substrate 2 (FRS2) suppresses TGF-β signaling via miRNA control.[112] FGFR1 may also inhibit EndMT by MAP4K4 antagonization of integrin β1-related TGF-β signaling.[113] Apart from TGF-β, Notch and Wnt/β-catenin signaling have also been implicated in EndMT.[114,115]

4.1.1 Mechanical stimuli in EndMT—Mechanical stimuli may provide direct EndMT signaling cues by the mechanisms described in previous sections, as well as tune the

sensitivity of ECs to biochemical stimuli such as TGF-β. TGF-β itself requires integrin binding of RGD sequences to mechanically unfold and activate latent stores in the ECM by force.[116] A number of mechanical contributors to the EndMT program have been covered in a recent review, with a focus on atherosclerosis.[117]

Flow: Egorova *et. al.* showed that cells lacking primary cilia, which can act as a mechanosensory component in low flow regions, were susceptible to shear-induced EndMT.[118] Kruppel-like factors KLF2 and KLF4 are involved in suppressing EndMT by inhibition of NFκB, reduced Smad2 and TGF-β signaling, and diminished ROS formation.[119] Low levels of 0.5 Pa shear applied to non-ciliated mutant mouse embryonic ECs induced EndMT in a TGF-β /ALK5-dependent manner, as indicated by loss of CD31 and upregulation of Snail, α−SMA, and N-cadherin. Shear-induced TGF-β signaling led to a loss of KLF4, but KLF4 overexpression, cilia rescue, or TGF-β receptor disruption could prevent shear-induced EndMT. These *in vitro* results corresponded well with in vivo observations of EndMT in low-shear regions of the vasculature of cilia-deficient mice.[118]

Transcriptome-wide analysis of differential gene expression at sequential time points during 24-hour exposure of HUVECs to pulsatile vs oscillatory flow provided a glimpse into the timeline of cell transitions. Oscillatory shear promoted significant downregulation of the EC genes such as endothelial nitric oxide synthase, vWF, and CD34 by six hours and upregulation of mesenchymal markers at 12 hours including cadherin-2 (CDH2), fibulin-5 (FBLN5), and tropomyosin α−1 chain (TPM1).[120] Oscillatory flow may instigate EndMT by disrupting the balance of FGF/ TGF-β signaling,[121] activating Twist/Gata4,[122] and promoting inflammatory signaling by NFκB.[120] Meanwhile, high laminar shear (2 Pa) seems to protect against EndMT by the MEK/ERK signaling pathway and Rac/Rho-mediated junctional stability.[117] ERK activation was found to confer protective effects by KLF-mediated suppression of EndMT related transcription factors and mesenchymal genes.[123] Low oscillatory shear of approximately 0.5 Pa applied to HUVECs within an orbital shaker was found to promote increased expression of Snail and mesenchymal markers Slug and N-cadherin as compared with those exposed to high 1.5 Pa uniform shear. The increased Snail expression was also apparent in atheroprone regions of murine aortas experiencing low wall shear stress and was downstream of Twist activation.[124] Together, these studies suggest involvement of EndMT in linking disturbed flow to inflammation and atherogenesis.[125]

Strain: HUVECs subjected to 10% cyclical stretch at 1Hz showed reversible progression towards a smooth muscle phenotype. These cells increased expression of adult smooth muscle marker SM22-α and α−SMA at the mRNA and protein levels after 48 hours, but these values recovered when cells were returned to static conditions.[126] Pathological stretch has been shown to activate Rho and destabilize junctions,[127] and upregulate MMP-1, MMP-2, and MMP-9,[128] which may each contribute to EndMT. Excessive stretch can also lead to production of ROS which enhances EndMT by oxidative stress, [109,129] and TGF-β upregulation by NLRP3 inflammasome activation.[130]

Stiffness: Matrix rigidity has a well-studied role in the related process of epithelial to mesenchymal transition (EMT),[131] though its contribution in EndMT is less thoroughly

examined. HUVECs cultured on stiff 491kPa PLL/HA multilayer films showed significant loss of endothelial markers vWF and CD31 after 2 weeks in the absence of growth factor supplements, while softer 317 kPa substrates promoted maintenance of the endothelial phenotype. Stimulation by TGF-β1 produced stiffness-dependent changes in morphology as cells became more elongated with increasing stiffness, as well as the appearance of the smooth muscle markers α−SMA and calponin.[132]

The transition of ECs to a mesenchymal-like phenotype produces corresponding changes in cellular biomechanical properties. Sancho *et. al.* used overexpression of MSX-1, a mediator of Bone Morphogenetic Protein 2 (BMP2)signaling,[133] in transfected HUAECs to induce EndMT. The transition was confirmed by reduced expression of CD31 and VE-cadherin and up-regulation of stem cell markers CD10 and CD90 and mesenchymal markers FSP-1, α-SMA, and Slug, as well as morphological elongation and flattening. MSX-1 overexpressing cells disassembled VE-cadherin and ZO1-stained cell-cell-junctions and became more polarized. These cells redistributed vinculin focal adhesions to the cell periphery at the ends of newly developed stress fibers. According, cells became stiffer as compared to controls. Using an AFM-based technique to quantify the difference between detachment force for single cells, compared to those in a monolayer, the group determined that MSX-1-induced EndMT reduced intercellular adhesion strength.[134] This is consistent with the observed cytoskeletal remodeling and reorganization of adhesions. Together, these and other studies point towards a link between matrix rigidity, cell stiffness, intracellular tension, and EndMT. In support of this connection, TGF-β activation of Smads activated Rho signaling to promote expression and nuclear accumulation of MRTF which lead to EndMT in mouse pancreatic microvascular ECs.[111]

As established in previous sections, RhoA signaling is enhanced in ECs on stiffer substrates.[85] RhoA activation by TGF-β and stiffness-induced nuclear twist accumulation are each drivers of mesenchymal transition in epithelial cells,[131,135] suggesting the possibility of similar mechanisms in EndMT. High stiffness also promotes activation of YAP/TAZ in vascular cells, [136] which interact with Snail and Slug in skeletal stem cells and regulate TGF-β/Smad signaling in fibroblasts.[137] While there may be also be relationship between spatial patterning cues and EMT via cytoskeletal organization,[138] more work would be needed to establish a definitive correlation in EndMT. Novel strategies for *in-vitro* recapitulation of EndMT, real time imaging of population transition dynamics, and studies of functional changes such as gain of contractile ability or loss of monocyte adhesiveness in addition to expression of cell markers may help to dissect the molecular mechanisms responsible for endothelial plasticity as well as the critical roles of mechanical stimuli. [125]

4.2 Tissue Engineering and Vascular Grafts

Cardiovascular disease is globally responsible for millions of deaths each year, with coronary artery occlusion representing roughly half of this number.[139] Vascular grafts can be used to bypass narrowed and obstructed vessels, and hundreds of thousands of these surgeries are performed each year in the United States.[140] Vascular grafts are commonly taken from another part of the patient's vasculature, such as the saphenous vein. However, a suitable replacement vessel is not always guaranteed, and the autologous graft may itself be

dysfunctional or prone to atherosclerosis. Mechanosensing also appears to play a role in failure of autologous grafts, for example by YAP/TAZ activation or Erk1/2 signaling.[141,142] Tissue engineered vascular grafts (TEVGs) may be used as alternative bypass conduits, but these approaches have not yet reached the success of autografts.[139] Major challenges in the performance of small diameter synthetic vascular grafts include thrombosis and intimal hyperplasia, or thickening of the tunica intima. These are generally caused by lack of a protective endothelium and a mismatch in mechanical properties between the graft and native vessel.[143] The inability to recapitulate these features often results in graft failure and low patency. Therefore, much focus has been placed on developing TEVGs which permit endothelialization of the surface while retaining mechanical integrity and compliance.[144]

In 1999, Niklason and Langer introduced the concept of pre-conditioning TEVGs with mechanical stimulation. They applied pulsatile flow for 8 weeks to bovine aortic SMCs seeded on biodegradable polyglycolic acid (PGA) scaffolds within bioreactors, then seeded BAECs on the inner lumen and continued to flow media at low 0.01–0.03 Pa shear for 3 days. The resulting engineered vessels showed greater rupture strength, suture retention, and more closely resembled the architecture of native vessels as compared to non-pulsed controls. Pulsed vessels implanted into the right saphenous artery of Yucatan miniature swine remained free of narrowing, while non-pulsed vessels developed thrombosis by three weeks. Several similar strategies have since emerged using biomimetic flow to improve graft mechanical properties.[145]

A multilayered 6-mm diameter graft consisting of three cell types isolated from bovine aortas was subjected to flow replicating that of aortic circulation, with pulsatile pressure and flow of 120/80mmHg and 1.4/0.2 L min^{-1}, respectively. ECs were seeded on the lumen of a 6 mm diameter tube consisting of SMCs and fibroblasts wrapped in polycaprolactone (PCL) and polyglycolic acid (PGA) sheets. ECs spread across the lumen and aligned with flow direction. These grafts had suitable rupture strength (827 kPa vs 882 kPa for native vessel) and elastic modulus (3.75 MPa vs 3.31 MPa for native vessel), with elastin production approaching that of native arteries.[146] Multilayered grafts containing synthetic human elastin and PCL exhibited similar elastic behavior and suitable burst pressures to internal mammary artery samples, as well as minimized coagulation and platelet adhesion and promoted EC attachment.[147]

While much focus has been placed on improving the graft bulk mechanical properties, scaffolds may also incorporate passive spatial cues to direct endothelial function. Suturable poly(vinyl alcohol) hydrogel (PVA) tubes with 2μm luminal gratings improved endothelialization and reduced thrombotic occlusion as compared to non-patterned grafts.[148] Electrospinning is a powerful tool commonly used to generate fibrous scaffolds mimicking the architecture and topography of native extracellular matrix,[149] and may be supplemented with further spatial patterning. Electrospun polyurethane (PU) scaffolds with longitudinally aligned 3.6 μm ridges of 0.9 μm height patterned on the luminal surface had a physiologically relevant longitudinal elastic modulus of 0.43 MPa. BAECs formed confluent monolayers with individual cells aligned along the grooves and remained responsive to TNF-α stimulation.[150] Pressed fibrous hyaluronan mats promoted adherence and

monolayer formation of human saphenous vein ECs over a 20 day period, as well as deposition of laminin, fibronectin, and collagen types IV and VIII.[151]

A large number of studies have demonstrated the potential of nanofibrous scaffolds in stimulating endothelial adhesion, proliferation, and functional gene expression.[152] Recently, however, Dong *et. al.* reported a smooth graft surface for enhanced hemocompatibility. HUVECs on smooth ultrathin PCL membranes showed reduced platelet adhesion and activation, quicker migration, enhanced monolayer formation and NO production as compared to randomly oriented nanofibrous (0.61 μm diameter) or microfibrous (9.9 μm diameter) substrates. Acellular hybrid vascular grafts with a smooth inner layer and a fibrous electrospun outer layer reduced thrombosis, platelet adhesion, and infiltration of plasma proteins in an arteriovenous shunt assay as compared to those with fibrous lumens.[153] Varied reports on the optimal degree of topographical patterning along with a diverse selection of reported materials may underscore the need for a more mechanistic approach.[154] A greater understanding and consideration of cell-substrate interactions in endothelial cell mechanobiology should facilitate rational design of effective tissue engineered scaffolds (Figure 4). It should be noted that this article covers a limited selection of approaches for tissue engineered vascular grafts, which have been reviewed in greater detail elsewhere. [139,155]

5. Future Outlook and Conclusion

ECs regulate the vascular environment by responding to a wide range of biophysical cues, including mechanical forces imposed by blood flow, passive properties of the ECM, and dynamic intercellular interactions. Accordingly, EC mechanosensing has contributed to our understanding of the progression of vascular diseases such as atherosclerosis. Although mechanotransduction has drawn the attention of numerous studies in recent years, further investigations are required to better understand the specific mechanosensing mechanisms by which ECs interpret complex signals in the vascular environment. Firstly, more complete and rigorous characterization of *in-vivo* mechanical properties is needed. This will require new tools and standardization of measurement techniques for both cell and substrate properties.[38] These results will inform the development of better engineered *in-vitro* biomimetic microenvironments.

Microfluidic organs-on chip can be used to study the synergistic effects of complex mechanical cues as well as co-culture with different cell types (e.g. smooth muscle cells and fibroblasts) on EC function.[156] Cell-cell interactions and biophysical signals present within these culture systems can reveal insights not apparent in simplified models.[157,158] Given the importance of substrate stiffness and shear stress in dictating EC mechanosignaling and function, future studies of endothelial mechanobiology would be well-advised to incorporate these stimuli at physiologically relevant levels. Ultimately, these biomimetic microsystems should allow for controlled application and quantification of mechanical perturbations on multiple scales. Platforms that facilitate advanced imaging and computational tools will feed into models of signal transduction linking the cytoskeleton to the nucleus and allow us to probe the mechanisms by which ECs translate physical cues into changes in behavior, gene expression, and epigenetics.

Unraveling the complexity of synergistic mechanical, biochemical and intercellular cues will require contributions from diverse disciplines from systems biology to biofabrication and biomaterials. The knowledge gained can be applied to disease models that enable the dissection and manipulation of dynamic pathological processes such as EndMT as they unfold. This can be further translated to the clinic through therapeutic targeting of mechanosensitive pathways implicated in vascular dysfunction, or by better replication of the *in-vivo* environment for tissue engineering and regenerative medicine.

Acknowledgements

This work was supported in part by grants to N.F.H. from the National Institutes of Health (R01 HL127113, R01 HL142718, and R21 EB020235), the Department of Veterans Affairs (1I01BX002310), the National Science Foundation (1829534), and the California Institute of Regenerative Medicine (10603).

Biography

Ngan F. Huang, PhD

Dr. Huang is an assistant professor of Cardiothoracic Surgery at Stanford University and principle investigator at the Center for Tissue Regeneration, Repair, and Restoration at Veterans Affairs Palo Alto Health Care System. Dr. Huang completed her BS in Chemical Engineering from the Massachusetts Institute of Technology, followed by a PhD in bioengineering from the University of California Berkeley and University of California San Francisco Joint Program in Bioengineering. Her research laboratory focuses on the role of chemical and mechanical interactions between the extracellular matrix and pluripotent stem cells that regulate cardiovascular differentiation and tissue regeneration

References

[1]. Chien S, AJP Hear. Circ. Physiol 2006, 292, H1209.

[2]. Eyckmans J, Boudou T, Yu X, Chen CS, Dev. Cell 2011, 21, 35. [PubMed: 21763607]

[3]. Sher M, Zhuang R, Demirci U, Asghar W, Expert Rev Mol Diagn 2017, 17, 351. [PubMed: 28103450]

[4]. Mendoza SA, Fang J, Gutterman DD, Wilcox DA, Bubolz AH, Li R, Suzuki M, Zhang DX, AJP Hear. Circ. Physiol 2010, 298, H466.

[5]. Wang SP, Chennupati R, Kaur H, Iring A, Wettschureck N, Offermanns S, J. Clin. Invest 2016, 126, 4527. [PubMed: 27797339]

[6]. Ranade SS, Qiu Z, Woo S-H, Hur SS, Murthy SE, Cahalan SM, Xu J, Mathur J, Bandell M, Coste B, Li Y-SJ, Chien S, Patapoutian A, Proc. Natl. Acad. Sci 2014, 111, 10347. [PubMed: 24958852]

[7]. Reitsma S, Slaaf DW, Vink H, Van Zandvoort MAMJ, Oude Egbrink MGA, Pflugers Arch. Eur. J. Physiol 2007, 454, 345. [PubMed: 17256154]

[8]. Weinbaum S, Zhang X, Han Y, Vink H, Cowin SC, Proc. Natl. Acad. Sci 2003, 100, 7988. [PubMed: 12810946]

[9]. Dragovich MA, Chester D, Fu BM, Wu C, Xu Y, Goligorsky MS, Zhang XF, Am. J. Physiol. - Cell Physiol 2016, 311, C846. [PubMed: 27681180]

[10]. Cooke JP, Proc. Natl. Acad. Sci 2003, 100, 768. [PubMed: 12552094]

[11]. Chachisvilis M, Zhang Y-L, Frangos JA, Proc. Natl. Acad. Sci 2006, 103, 15463. [PubMed: 17030791]

[12]. Jacobs CR, Huang H, Kwon RY, Introduction to Cell Mechanics and Mechanobiology; Garland Science: New York, NY, USA, 2012.

[13]. Sinha B, Köster D, Ruez R, Gonnord P, Bastiani M, Abankwa D, Stan RV, Butler-Browne G, Vedie B, Johannes L, Morone N, Parton RG, Raposo G, Sens P, Lamaze C, Nassoy P, Cell 2011, 144, 402. [PubMed: 21295700]

[14]. Qi Y, Andolfi L, Frattini F, Mayer F, Lazzarino M, Hu J, Nat. Commun 2015, 6.

[15]. Sun X, Fu Y, Gu M, Zhang L, Li D, Li H, Chien S, Shyy JY-J, Zhu Y, Proc. Natl. Acad. Sci 2016, 113, 769. [PubMed: 26733684]

[16]. Humphrey JD, Schwartz MA, Tellides G, Milewicz DM, Circ. Res 2015, 116, 1448. [PubMed: 25858068]

[17]. Galbraith CG, Yamada KM, Sheetz MP, J. Cell Biol 2002, 159, 695. [PubMed: 12446745]

[18]. del Rio A, Perez-Jimenez R, Liu R, Rosa-Cusachs P, Fernandez JM, Sheetz MP, Science. 2009, 323, 638. [PubMed: 19179532]

[19]. Le S, Hu X, Yao M, Chen H, Yu M, Xu X, Nakazawa N, Margadant FM, Sheetz MP, Yan J, Cell Rep. 2017, 21, 2714. [PubMed: 29212020]

[20]. Ridley AJ, Trends Cell Biol. 2006, 16, 522. [PubMed: 16949823]

[21]. Bhadriraju K, Yang M, Alom Ruiz S, Pirone D, Tan J, Chen CS, Exp. Cell Res 2007, 313, 3616. [PubMed: 17673200]

[22]. Huveneers S, Daemen MJAP, Hordijk PL, Circ. Res 2015, 116, 895. [PubMed: 25722443]

[23]. Kiosses WB, Shattil SJ, Pampori N, Schwartz MA, Nat. Cell Biol 2001, 3, 316. [PubMed: 11231584]

[24]. Goldmann WH, Ingber DE, Biochem. Biophys. Res. Commun 2002, 290, 749. [PubMed: 11785963]

[25]. Xia N, Thodeti CK, Hunt TP, Xu Q, Ho M, Whitesides GM, Westervelt R, Ingber DE, FASEB J. 2008, 22, 1649. [PubMed: 18180334]

[26]. Zhou J, Li Y-S, Chien S, Arterioscler. Thromb. Vasc. Biol 2014, 34, 2191. [PubMed: 24876354]

[27]. Vicente-Manzanares M, Ma X, Adelstein RS, Horwitz AR, Nat. Rev. Cell Biol 2009, 10, 778.

[28]. Geiger B, Spatz JP, Bershadsky AD, Nat. Rev. Mol. Cell Biol 2009, 10, 21. [PubMed: 19197329]

[29]. Wolfenson H, Meacci G, Liu S, Stachowiak MR, Iskratsch T, Ghassemi S, Roca-Cusachs P, O'Shaughnessy B, Hone J, Sheetz MP, Nat. Cell Biol 2016, 18, 33. [PubMed: 26619148]

[30]. Tzima E, Irani-Tehrani M, Kiosses WB, Dejana E, Schultz DA, Engelhardt B, Cao G, DeLisser H, Schwartz MA, Nature 2005, 437, 426. [PubMed: 16163360]

[31]. Barry AK, Wang N, Leckband DE, J. Cell Sci 2015, 128, 1341. [PubMed: 25663699]

[32]. Collins C, Guilluy C, Welch C, O'Brien ET, Hahn K, Superfine R, Burridge K, Tzima E, Curr. Biol 2012, 22, 2087. [PubMed: 23084990]

[33]. Vogel V, Sheetz M, Nat. Rev. Mol. Cell Biol 2006, 7, 265. [PubMed: 16607289]

[34]. Wang N, Butler JP, Ingber DE, Science. 1993, 260, 1124. [PubMed: 7684161]

[35]. Maniotis AJ, Chen CS, Ingber DE, Proc. Natl. Acad. Sci 1997, 94, 849. [PubMed: 9023345]

[36]. Na S, Collin O, Chowdhury F, Tay B, Ouyang M, Wang Y, Wang N, Proc. Natl. Acad. Sci 2008, 105, 6626. [PubMed: 18456839]

[37]. Crisp M, Liu Q, Roux K, Rattner JB, Shanahan C, Burke B, Stahl PD, Hodzic D, J. Cell Biol 2006, 172, 41. [PubMed: 16380439]

[38]. Holle AW, Young JL, Van Vliet KJ, Kamm RD, Discher D, Janmey P, Spatz JP, Saif T, Nano Lett. 2018, 18, 1. [PubMed: 29178811]

[39]. Dupont S, Morsut L, Aragona M, Enzo E, Giulitti S, Cordenonsi M, Zanconato F, Le Digabel J, Forcato M, Bicciato S, Elvassore N, Piccolo S, Nature 2011, 474, 179. [PubMed: 21654799]

[40]. Wang K-C, Yeh Y-T, Nguyen P, Limqueco E, Lopez J, Thorossian S, Guan K-L, Li Y-SJ, Chien S, Proc. Natl. Acad. Sci 2016, 113, 11525. [PubMed: 27671657]

[41]. Choi HJ, Zhang H, Park H, Choi KS, Lee HW, Agrawal V, Kim YM, Kwon YG, Nat. Commun 2015, 6.

[42]. Serrano I, McDonald PC, Lock F, Muller WJ, Dedhar S, Nat. Commun 2013, 4.

[43]. Yu FX, Zhao B, Panupinthu N, Jewell JL, Lian I, Wang LH, Zhao J, Yuan H, Tumaneng K, Li H, Fu XD, Mills GB, Guan KL, Cell 2012, 150, 780. [PubMed: 22863277]

[44]. Jiang YZ, Manduchi E, Jiménez JM, Davies PF, Arterioscler. Thromb. Vasc. Biol 2015, 35, 1317. [PubMed: 25838424]

[45]. Qin X, Wang X, Wang Y, Tang Z, Cui Q, Xi J, Li Y-SJ, Chien S, Wang N, Proc. Natl. Acad. Sci 2010, 107, 3240. [PubMed: 20133739]

[46]. Lee D-Y, Lin T-E, Lee C-I, Zhou J, Huang Y-H, Lee P-L, Shih Y-T, Chien S, Chiu J-J, Proc. Natl. Acad. Sci 2017, 114, 2072. [PubMed: 28167758]

[47]. Kumar S, Kim CW, Simmons RD, Jo H, Arterioscler. Thromb. Vasc. Biol 2014, 34, 2206. [PubMed: 25012134]

[48]. Lee D-Y, Lee C-I, Lin T-E, Lim SH, Zhou J, Tseng Y-C, Chien S, Chiu J-J, Proc. Natl. Acad. Sci 2012, 109, 1967. [PubMed: 22308472]

[49]. Zhou J, Li YS, Wang KC, Chien S, Cell. Mol. Bioeng 2014, 7, 218. [PubMed: 24883126]

[50]. Portela A, Esteller M, Nat. Biotechnol 2010, 28, 1057. [PubMed: 20944598]

[51]. Malek AM, Alper SL, Izumo S, JAMA 1999, 282, 2035. [PubMed: 10591386]

[52]. Baeyens N, Bandyopadhyay C, Coon BG, Yun S, Schwartz MA, J. Clin. Invest 2016, 126, 821. [PubMed: 26928035]

[53]. Andresen Eguiluz RC, Kaylan KB, Underhill GH, Leckband DE, Biomaterials 2017, 140, 45. [PubMed: 28624707]

[54]. Thubrikar MJ, Robicsek F, Ann. Thorac. Surg 1995, 59, 1594. [PubMed: 7771858]

[55]. Davies PF, Civelek M, Fang Y, Guerraty MA, Passerini AG, Semin. Thromb. Hemost 2010, 36, 265. [PubMed: 20533180]

[56]. Kataoka N, Ujita S, Sato M, Med. Biol. Eng. Comput 1998, 36, 122. [PubMed: 9614760]

[57]. Levesque MJ, Nerem RM, J Biomech Eng 1985, 107, 341. [PubMed: 4079361]

[58]. Galbraith CG, Skalak R, Chien S, Cell Motil. Cytoskeleton 1998, 40, 317. [PubMed: 9712262]

[59]. Chien S, Ann. Biomed. Eng 2008, 36, 554. [PubMed: 18172767]

[60]. Davies PF, Remuzzi A, Gordon EJ, Dewey CF, Gimbrone MA, Proc. Natl. Acad. Sci. U. S. A 1986, 83, 2114. [PubMed: 3457378]

[61]. Chiu JJ, Wang DL, Chien S, Skalak R, Usami S, J Biomech Eng 1998, 120, 2. [PubMed: 9675673]

[62]. Miao H, Hu Y-L, Shiu Y-T, Yuan S, Zhao Y, Kaunas R, Wang Y, Jin G, Usami S, Chien S, J. Vasc. Res 2005, 42, 77. [PubMed: 15637443]

[63]. Conway DE, Breckenridge MT, Hinde E, Gratton E, Chen CS, Schwartz MA, Curr Biol. 2013, 23, 1024. [PubMed: 23684974]

[64]. Tkachenko E, Gutierrez E, Saikin SK, Fogelstrand P, Kim C, Groisman A, Ginsberg MH, Biol. Open 2013, 2, 1007. [PubMed: 24167710]

[65]. Chen CS, Mrksich M, Huang S, Whitesides GM, Ingber DE, Science. 1997, 276, 1425. [PubMed: 9162012]

[66]. Dike LE, Chen CS, Mrksich M, Tien J, Whitesides GM, Ingber DE, Vitr. Cell. Dev. Biol. - Anim 1999, 35, 441.

[67]. Li S, Bhatia S, Hu YL, Shiu YT, Li YS, Usami S, Chien S, Biorheology 2001, 38, 101. [PubMed: 11381168]

[68]. Parker KK, Brock AL, Brangwynne C, Mannix RJ, Wang N, Ostuni E, Geisse NA, Adams JC, Whitesides GM, Ingber DE, FASEB J. 2002, 16, 1195. [PubMed: 12153987]

[69]. Bettinger CJ, Orrick B, Misra A, Langer R, Borenstein JT, Biomaterials 2006, 27, 2558. [PubMed: 16386300]

[70]. Lu J, Rao MP, MacDonald NC, Khang D, Webster TJ, Acta Biomater. 2008, 4, 192. [PubMed: 17851147]

[71]. Bettinger CJ, Zhang Z, Gerecht S, Borenstein JT, Langer R, Adv. Mater 2008, 20, 99. [PubMed: 19440248]

[72]. Lai ES, Huang NF, Cooke JP, Fuller GG, Regen. Med 2012, 7, 649. [PubMed: 22954436]

[73]. Sundararaghavan HG, Saunders RL, Hammer DA, Burdick JA, Biotechnol. Bioeng 2013, 110, 1249. [PubMed: 23172355]

[74]. Nakayama KH, Surya VN, Gole M, Walker TW, Yang W, Lai ES, Ostrowski MA, Fuller GG, Dunn AR, Huang NF, Nano Lett. 2016, 16, 410. [PubMed: 26670737]

[75]. Discher DE, Janmey P, Wang YL, Science. 2005, 310, 1139. [PubMed: 16293750]

[76]. Engler AJ, Sen S, Sweeney HL, Discher DE, Cell 2006, 126, 677. [PubMed: 16923388]

[77]. Yeung T, Georges PC, Flanagan LA, Marg B, Ortiz M, Funaki M, Zahir N, Ming W, Weaver V, Janmey PA, Cell Motil. Cytoskeleton 2005, 60, 24. [PubMed: 15573414]

[78]. Engler AJ, Richert L, Wong JY, Picart C, Discher DE, Surf. Sci 2004, 570, 142.

[79]. Klein EA, Yin L, Kothapalli D, Castagnino P, Byfield FJ, Xu T, Levental I, Hawthorne E, Janmey PA, Assoian RK, Curr. Biol 2009, 19, 1511. [PubMed: 19765988]

[80]. Peloquin J, Huynh J, Williams RM, Reinhart-King CA, J. Biomech 2011, 44, 815. [PubMed: 21288524]

[81]. Huynh J, Nishimura N, Rana K, Peloquin JM, Califano JP, Montague CR, King MR, Schaffer CB, Reinhart-King CA, Sci. Transl. Med 2011, 3, 112ra122.

[82]. Redfield MM, Jacobsen SJ, Borlaug BA, Rodeheffer RJ, Kass DA, Circulation 2005, 112, 2254. [PubMed: 16203909]

[83]. Matsumoto T, Abe H, Ohashi T, Kato Y, Sato M, Physiol. Meas 2002, 23, 635. [PubMed: 12450265]

[84]. Callister WD, Fundamentals of Materials Science and Engineering: An Interactive E-Text; 5th ed.; John Wiley & Sons, Inc.: Somerset, NJ, 2000.

[85]. Yeh YT, Hur SS, Chang J, Wang KC, Chiu JJ, Li YS, Chien S, PLoS One 2012, 7, 46889.

[86]. Canver AC, Ngo O, Urbano RL, Clyne AM, J. Biomech 2016, 49, 1369. [PubMed: 26792289]

[87]. Reinhart-King CA, Dembo M, Hammer DA, Biophys. J 2005, 89, 676. [PubMed: 15849250]

[88]. Califano JP, Reinhart-King CA, Cell. Mol. Bioeng 2010, 3, 68. [PubMed: 21116436]

[89]. Krishnan R, Klumpers DD, Park CY, Rajendran K, Trepat X, van Bezu J, van Hinsbergh VWM, V Carman C, Brain JD, Fredberg JJ, Butler JP, van Nieuw Amerongen GP, AJP Cell Physiol 2011, 300, C146.

[90]. Stroka KM, Aranda-Espinoza H, Blood 2011, 118, 1632. [PubMed: 21652678]

[91]. Kohn JC, Chen A, Cheng S, Kowal DR, King MR, Reinhart-King CA, J. Biomech 2016, 49, 1447. [PubMed: 27020750]

[92]. Lampi MC, Guvendiren M, Burdick JA, Reinhart-King CA, ACS Biomater. Sci. Eng 2017, 3, 3007.

[93]. Galie PA, Van Oosten A, Chen CS, Janmey PA, Lab Chip 2015, 15, 1205. [PubMed: 25573790]

[94]. Anwar MA, Shalhoub J, Lim CS, Gohel MS, Davies AH, J. Vasc. Res 2012, 49, 463. [PubMed: 22796658]

[95]. Wang BW, Chang H, Lin S, Kuan P, Shyu KG, Cardiovasc. Res 2003, 59, 460. [PubMed: 12909329]

[96]. Carosi JA, Eskin SG, McIntire LV, J. Cell. Physiol 1992, 151, 29. [PubMed: 1560046]

[97]. Jufri NF, Mohamedali A, Avolio A, Baker MS, Vasc. Cell 2015, 7, 8. [PubMed: 26388991]

[98]. Iba T, Sumpio BE, Microvasc. Res 1991, 42, 245. [PubMed: 1779881]

[99]. Wang JHC, Goldschmidt-Clermont P, Wille J, Yin FCP, J. Biomech 2001, 34, 1563. [PubMed: 11716858]

[100]. Liu XM, Ensenat D, Wang H, Schafer AI, Durante W, FEBS Lett. 2003, 541, 52. [PubMed: 12706818]

[101]. Yano Y, Geibel J, Sumpio BE, Am J Physiol 1996, 271, 635.

[102]. Thodeti CK, Matthews B, Ravi A, Mammoto A, Ghosh K, Bracha AL, Ingber DE, Circ. Res 2009, 104, 1123. [PubMed: 19359599]

[103]. Medici D, Shore EM, Lounev VY, Kaplan FS, Kalluri R, Olsen BR, Nat. Med 2010, 16, 1400. [PubMed: 21102460]

[104]. Medici D, Kalluri R, Semin. Cancer Biol 2012, 22, 379. [PubMed: 22554794]

[105]. Armstrong EJ, Bischoff J, Circ. Res 2004, 95, 459. [PubMed: 15345668]

[106]. Arciniegas E, Frid MG, Douglas IS, Stenmark KR, Am. J. Physiol. Cell. Mol. Physiol 2007, 293, L1.

[107]. Van Meeteren LA, Ten Dijke P, Cell Tissue Res. 2012, 347, 177. [PubMed: 21866313]

[108]. Zeisberg EM, Potenta S, Xie L, Zeisberg M, Kalluri R, Cancer Res. 2007, 67, 10123. [PubMed: 17974953]

[109]. Evrard SM, Lecce L, Michelis KC, Nomura-Kitabayashi A, Pandey G, Purushothaman KR, D'Escamard V, Li JR, Hadri L, Fujitani K, Moreno PR, Benard L, Rimmele P, Cohain A, Mecham B, Randolph GJ, Nabel EG, Hajjar R, Fuster V, Boehm M, Kovacic JC, Nat. Commun 2016, 7, 11853. [PubMed: 27340017]

[110]. Zeisberg EM, Tarnavski O, Zeisberg M, Dorfman AL, McMullen JR, Gustafsson E, Chandraker A, Yuan X, Pu WT, Roberts AB, Neilson EG, Sayegh MH, Izumo S, Kalluri R, Nat. Med 2007, 13, 952. [PubMed: 17660828]

[111]. Mihira H, Suzuki HI, Akatsu Y, Yoshimatsu Y, Igarashi T, Miyazono K, Watabe T, J. Biochem 2012, 151, 145. [PubMed: 21984612]

[112]. Chen PY, Qin L, Barnes C, Charisse K, Yi T, Zhang X, Ali R, Medina PP, Yu J, Slack FJ, Anderson DG, Kotelianski V, Wang F, Tellides G, Simons M, Cell Rep. 2012, 2, 1684. [PubMed: 23200853]

[113]. Li J, Shi S, Srivastava SP, Kitada M, Nagai T, Nitta K, Kohno M, Kanasaki K, Koya D, Cell Death Dis. 2017, 8, e2965. [PubMed: 28771231]

[114]. Niessen K, Fu YX, Chang L, Hoodless PA, McFadden D, Karsan A, J. Cell Biol 2008, 182, 315. [PubMed: 18663143]

[115]. Aisagbonhi O, Rai M, Ryzhov S, Atria N, Feoktistov I, Hatzopoulos AK, Dis. Model. Mech 2011, 4, 469. [PubMed: 21324930]

[116]. Shi M, Zhu J, Wang R, Chen X, Mi L, Walz T, Springer TA, Nature 2011, 474, 343. [PubMed: 21677751]

[117]. Souilhol C, Harmsen MC, Evans PC, Krenning G, Cardiovasc. Res 2018, 114, 565. [PubMed: 29309526]

[118]. Egorova AD, Khedoe PPSJ, Goumans M-JJTH, Yoder BK, Nauli SM, Ten Dijke P, Poelmann RE, Hierck BP, Circ. Res 2011, 108, 1093. [PubMed: 21393577]

[119]. Krenning G, Barauna VG, Krieger JE, Harmsen MC, Moonen J-RRAJ, Endothelial Plasticity: Shifting Phenotypes through Force Feedback. Stem Cells Int. 2016, 2016.

[120]. Ajami NE, Gupta S, Maurya MR, Nguyen P, Li JY-S, Shyy JY-J, Chen Z, Chien S, Subramaniam S, Proc. Natl. Acad. Sci 2017, 114, 10990. [PubMed: 28973892]

[121]. Chen PY, Qin L, Baeyens N, Li G, Afolabi T, Budatha M, Tellides G, Schwartz MA, Simons M, J. Clin. Invest 2015, 125, 4514. [PubMed: 26517696]

[122]. Mahmoud MM, Kim HR, Xing R, Hsiao S, Mammoto A, Chen J, Serbanovic-Canic J, Feng S, Bowden NP, Maguire R, Ariaans M, Francis SE, Weinberg PD, Van Der Heiden K, Jones EA, Chico TJA, Ridger V, Evans PC, Circ. Res 2016, 119, 450. [PubMed: 27245171]

[123]. Moonen JRAJ, Lee ES, Schmidt M, Maleszewska M, Koerts JA, Brouwer LA, Van Kooten TG, Van Luyn MJA, Zeebregts CJ, Krenning G, Harmsen MC, Cardiovasc. Res 2015, 108, 377. [PubMed: 26084310]

[124]. Mahmoud MM, Serbanovic-Canic J, Feng S, Souilhol C, Xing R, Hsiao S, Mammoto A, Chen J, Ariaans M, Francis SE, Van Der Heiden K, Ridger V, Evans PC, Sci. Rep 2017, 7, 3375. [PubMed: 28611395]

[125]. Li Y, Lui KO, Zhou B, Nat. Rev. Cardiol 2018, 15, 445. [PubMed: 29748594]

[126]. Cevallos M, Riha GM, Wang X, Yang H, Yan S, Li M, Chai H, Yao Q, Chen C, Differentiation 2006, 74, 552. [PubMed: 17177852]

[127]. Birukov KG, Jacobson JR, Flores A-DA, Ye SQ, Birukova AA, Verin AD, Garcia JGN, Am. J. Physiol. Cell. Mol. Physiol 2003, 285, L785.

[128]. Balachandran K, Sucosky P, Jo H, Yoganathan AP, AJP Hear. Circ. Physiol 2009, 296, H756.

[129]. Ali MH, Pearlstein DP, Mathieu CE, Schumacker PT, Am. J. Physiol. Lung Cell. Mol. Physiol 2004, 287, L486. [PubMed: 15090367]

[130]. Lv Z, Wang Y, Liu YJ, Mao YF, Dong WW, Ding ZN, Meng GX, Jiang L, Zhu XY, Crit. Care Med 2018, 46, e49. [PubMed: 29088003]

[131]. Wei SC, Fattet L, Tsai JH, Guo Y, Pai VH, Majeski HE, Chen AC, Sah RL, Taylor SS, Engler AJ, Yang J, Nat. Cell Biol. 2015, 17, 678. [PubMed: 25893917]

[132]. Zhang H, Chang H, Wang LM, Ren KF, Martins CML, Barbosa MA, Ji J, Biomacromolecules 2015, 16, 3584. [PubMed: 26477358]

[133]. Ma L, Lu M-F, Schwartz RJ, Martin JF, Development 2005, 132, 5601. [PubMed: 16314491]

[134]. Sancho A, Vandersmissen I, Craps S, Luttun A, Groll J, Sci. Rep 2017, 7, 46152. [PubMed: 28393890]

[135]. Bhowmick NA, Ghiassi M, Bakin A, Aakre M, Lundquist CA, Engel ME, Arteaga CL, Moses HL, Mol. Biol. Cell 2001, 12, 27. [PubMed: 11160820]

[136]. Bertero T, Fessel J, Chan SY, J Clin Invest 2016, 126, 3313. [PubMed: 27548520]

[137]. Tang Y, Feinberg T, Keller ET, Li XY, Weiss SJ, Nat. Cell Biol 2016, 18, 917. [PubMed: 27479603]

[138]. Nasrollahi S, Pathak A, Sci. Rep 2016, 6. [PubMed: 28442741]

[139]. Seifu DG, Purnama A, Mequanint K, Mantovani D, Nat. Rev. Cardiol 2013, 10, 410. [PubMed: 23689702]

[140]. Pashneh-Tala S, MacNeil S, Claeyssens F, Tissue Eng. Part B Rev 2016, 22, 68. [PubMed: 26447530]

[141]. Ruiter MS, Pesce M, Front. Cardiovasc. Med 2018, 5. [PubMed: 29445728]

[142]. Fischer PF, J. Biomech. Eng 2003, 125, 49. [PubMed: 12661196]

[143]. Zilla P, Bezuidenhout D, Human P, Biomaterials 2007, 28, 5009. [PubMed: 17688939]

[144]. Salacinski HJ, Goldner S, Giudiceandrea A, Hamilton G, Seifalian AM, Edwards A, Carson RJ, J. Biomater. Appl 2001, 15, 241. [PubMed: 11261602]

[145]. Niklason LE, Gao J, Abbott WM, Hirschi KK, Houser S, Marini R, Langer R, Science. 1999, 284, 489. [PubMed: 10205057]

[146]. Iwasaki K, Kojima K, Kodama S, Paz AC, Chambers M, Umezu M, Vacanti CA, Circulation 2008, 118, S52. [PubMed: 18824769]

[147]. Wise SG, Byrom MJ, Waterhouse A, Bannon PG, Ng MKC, Weiss AS, Acta Biomater. 2011, 7, 295. [PubMed: 20656079]

[148]. Cutiongco MF, Goh SH, Aid-Launais R, Le Visage C, Low HY, Yim EK, Biomaterials 2016, 84, 184. [PubMed: 26828683]

[149]. Hasan A, Memic A, Annabi N, Hossain M, Paul A, Dokmeci MR, Dehghani F, Khademhosseini A, Acta Biomater. 2014, 10, 11. [PubMed: 23973391]

[150]. Uttayarat P, Perets A, Li M, Pimton P, Stachelek SJ, Alferiev I, Composto RJ, Levy RJ, Lelkes PI, Acta Biomater. 2010, 6, 4229. [PubMed: 20601235]

[151]. Turner NJ, Kielty CM, Walker MG, Canfield AE, Biomaterials 2004, 25, 5955. [PubMed: 15183610]

[152]. Sankaran KK, Subramanian A, Krishnan UM, Sethuraman S, Biotechnol. J 2015, 10, 96. [PubMed: 25641941]

[153]. Dong X, Yuan X, Wang L, Liu J, Midgley AC, Wang Z, Wang K, Liu J, Zhu M, Kong D, Biomaterials 2018, 181, 1. [PubMed: 30056334]

[154]. Li X, Wang X, Yao D, Jiang J, Guo X, Gao Y, Li Q, Shen C, Colloids Surfaces B Biointerfaces 2018, 171, 461. [PubMed: 30077146]

[155]. Melchiorri AJ, Hibino N, Fisher JP, Tissue Eng. Part B Rev 2013, 19, 292. [PubMed: 23252992]

[156]. Bhatia SN, Ingber DE, Nat. Biotechnol 2014, 32, 760. [PubMed: 25093883]

[157]. Alimperti S, Mirabella T, Bajaj V, Polacheck W, Pirone DM, Duffield J, Eyckmans J, Assoian RK, Chen CS, Proc. Natl. Acad. Sci 2017, 114, 8758. [PubMed: 28765370]

[158]. Gray KM, Stroka KM, Semin. Cell Dev. Biol 2017, 71, 106. [PubMed: 28633977]

[159]. G. D, M.R. K-M, S. N, Y. Z, S. V, B.R. B, R.D. K, G. G-C, M.A. GJ, Proc. Natl. Acad. Sci. U. S. A 2004, 101, 14871. [PubMed: 15466704]

[160]. Byfield FJ, Reen RK, Shentu TP, Levitan I, Gooch KJ, J. Biomech 2009, 42, 1114. [PubMed: 19356760]

[161]. Sieminski AL, Hebbel RP, Gooch KJ, Exp. Cell Res 2004, 297, 574. [PubMed: 15212957]

[162]. Rao RR, Peterson AW, Ceccarelli J, Putnam AJ, Stegemann JP, Angiogenesis 2012, 15, 253. [PubMed: 22382584]

[163]. Yung YC, Chae J, Buehler MJ, Hunter CP, Mooney DJ, Proc. Natl. Acad. Sci. U. S. A 2009, 106, 15279. [PubMed: 19706407]

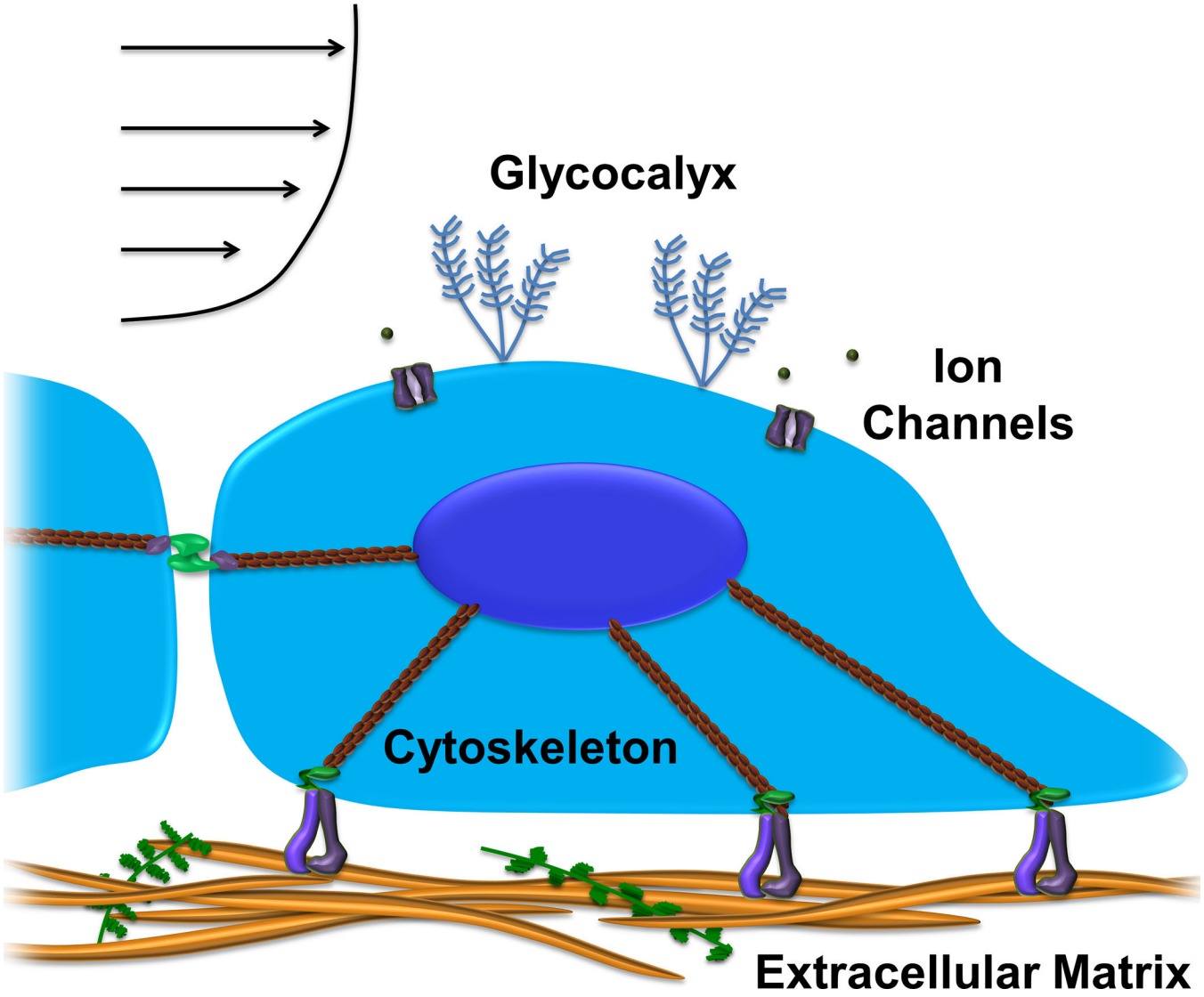

Figure 1. A complex, organized mechanotransduction system integrates mechanical signals in the endothelial environment.

Components of the mechanosensory network include ion channels, the glycocalyx, cell-ECM adhesions, intercellular junctions, and the cytoskeleton.

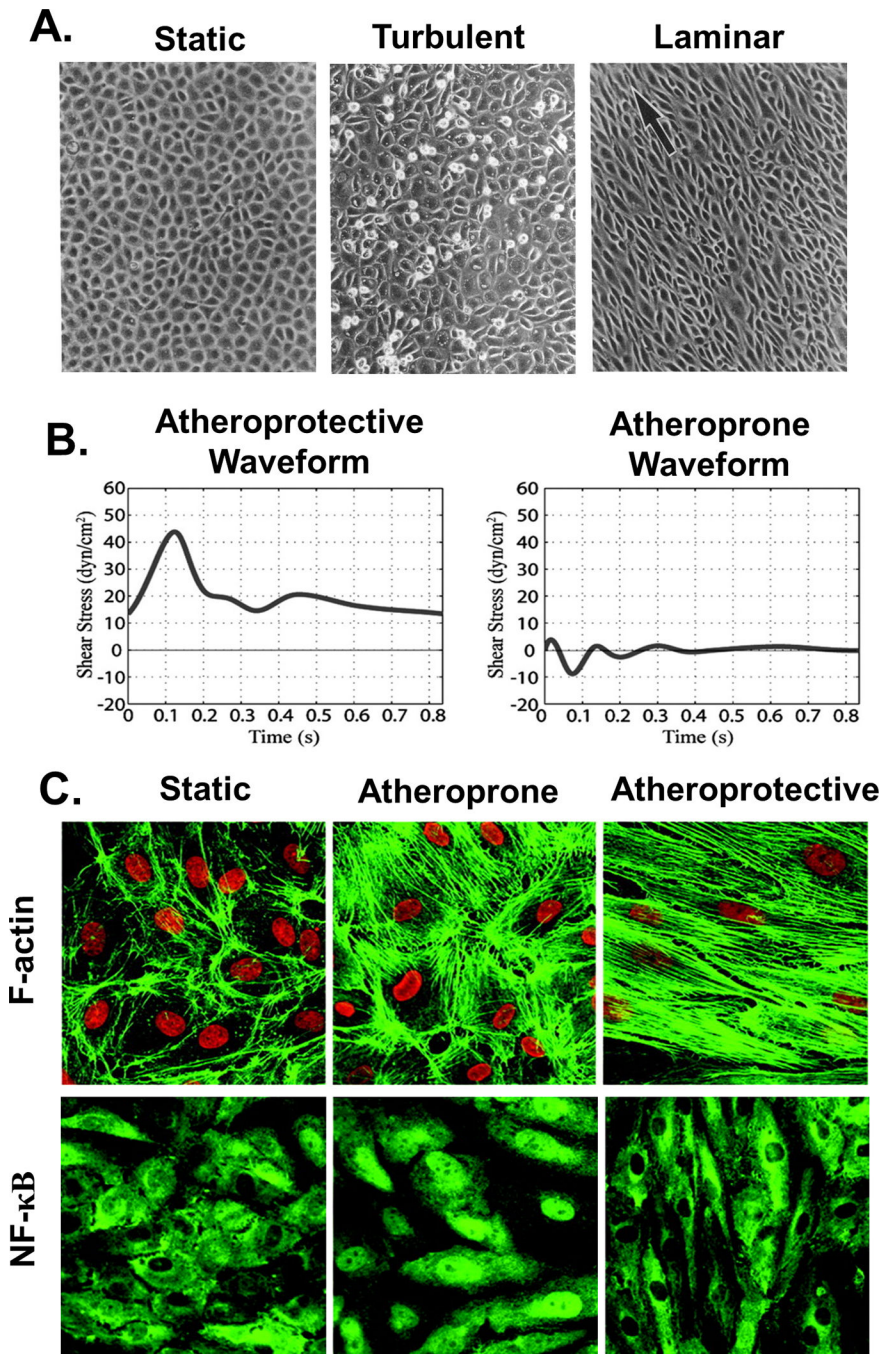

Figure 2. Endothelial monolayer responses to fluid shear stress.

A. Bovine aortic endothelial cells (BAECs) in a confluent monolayer under static conditions (left) exhibit a polygonal configuration with no preferred orientation. ECs exposed to 16 hours of turbulent 0.15 Pa flow (middle) show variable cell shape, lack of alignment, and significant cell rounding. Monolayers after 24 hours of exposure to 0.8 Pa laminar flow (right) show alignment with the direction of flow, indicated by the arrow. Adapted with permission from [60]. **B.** Representative atheroprotective (left) and atheroprone (right) waveforms were generated from computational simulations of flow patterns in human

carotid arteries. **C.** HUVEC cytoskeletal organization after 24h exposure to static (left), atheroprone (middle), or atheroprotective (right) waveforms generated using a dynamic cone and plate flow system. Atheroprone waveforms enhanced NF-κB nuclear translocation. B&C Adapted with permission from [159]. Copyright 2004 National Academy of Sciences.

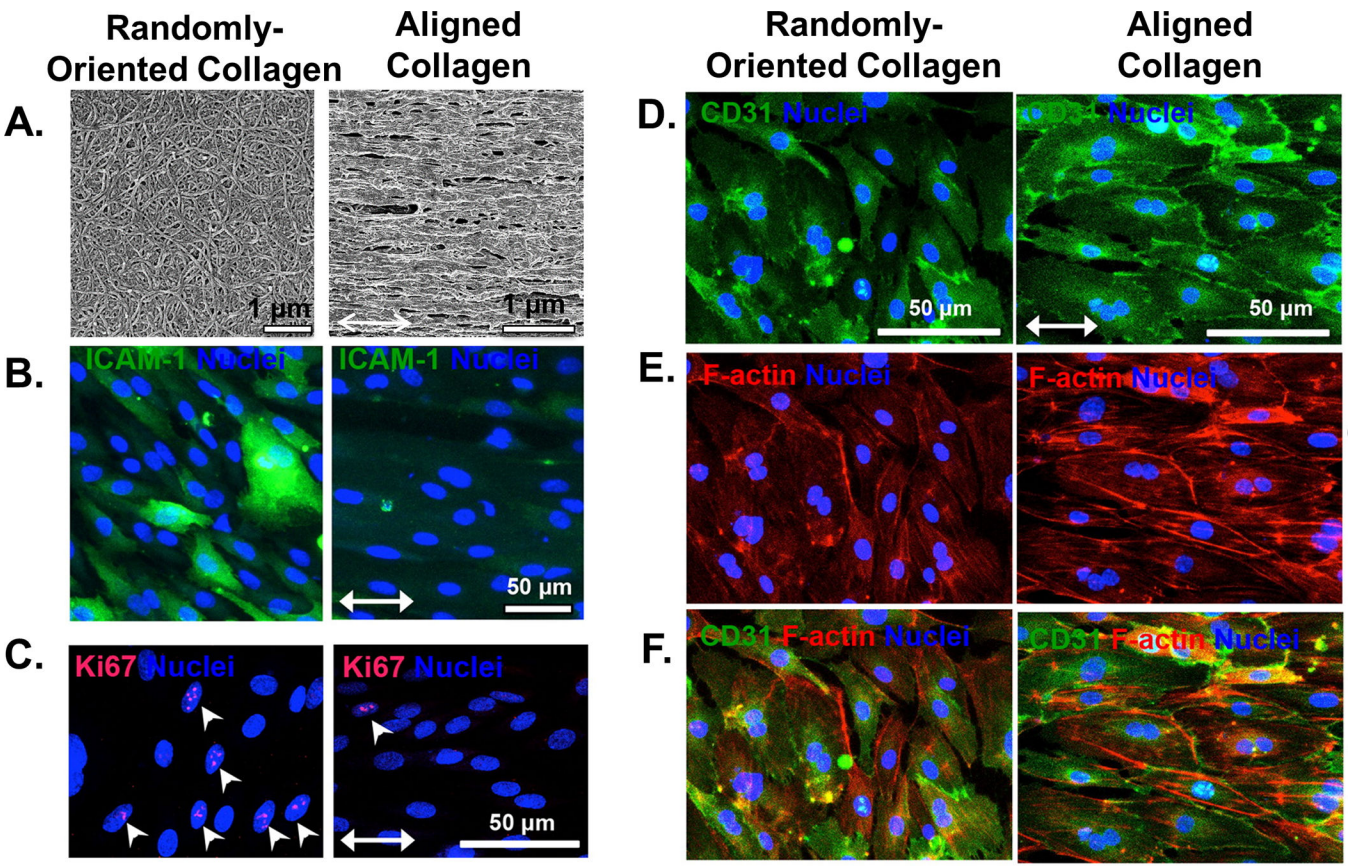

Figure 3. Aligned nanofibrillar collagen films regulate proliferation, inflammatory properties, junctional thickness, and cytoskeletal organization in primary human dermal microvascular ECs despite exposure to spatially varying fluid shear stress.

A. Randomly-oriented vs. parallel-aligned nanofibrillar collagen films generated by shear-mediated extrusion. **B.** Aligned scaffolds downregulate expression of ICAM-1, an inflammatory adhesion molecule. **C.** Aligned scaffolds reduce the fractions of Ki67 expressing cells, indicating reduced EC turnover. **D-F.** Aligned scaffolds promote CD31 junctional thickness (D), cytoskeletal organization and elongation along the direction of anisotropy (E), as shown by merged images (F). Adapted with permission from [74]. Copyright 2016 American Chemical Society.

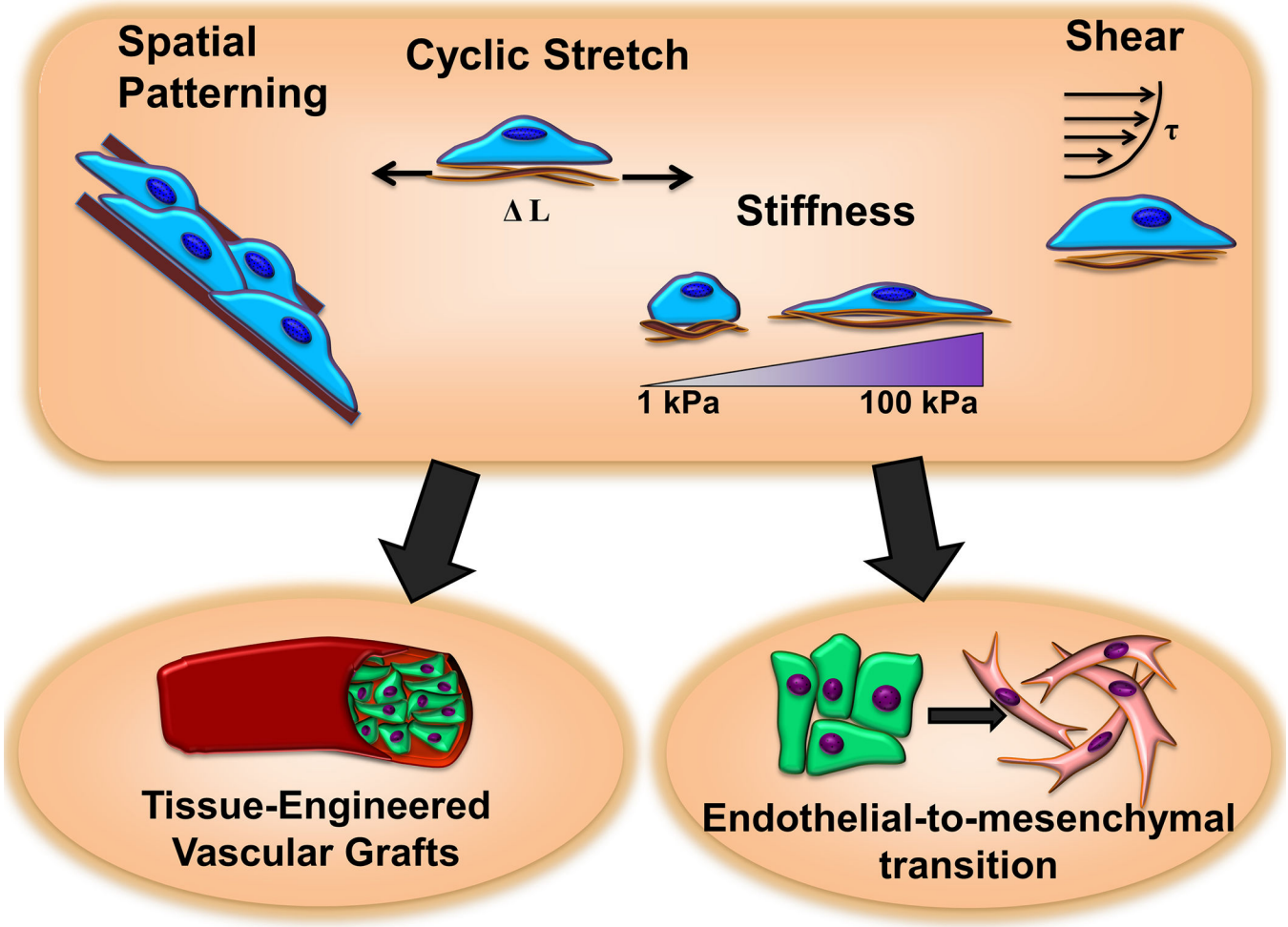

Figure 4. Mechanical forces and extracellular matrix properties provide essential cues to regulate the process of endothelial-to-mesenchymal transition.

The knowledge gained can inform the design of tissue-engineered vascular grafts.

Table 1.

Passive mechanical and geometric cues derived from extracellular matrix interactions direct endothelial cell (EC) behavior and function

Mechanical Stimulus	Cell Type	Stimulus Parameters	Results	Reference
Micropatterning	Bovine capillary EC	Square patterns, 75 to 3000 μm^2	Increased DNA synthesis and reduced apoptosis with greater spreading	[65]
Micropatterning	Bovine capillary EC	10 and 30 μm-width lines	Capillary tube formation and ECM fibril remodeling on 10 μm columns	[66]
Micropatterning	Bovine aortic EC	15, 30 and 60 μm-width lines	Greater elongation and alignment, reduced spreading, higher migration speeds, and more persistent directional migration on 10 μm columns	[67]
Micropatterning	Bovine capillary EC	Square and round patterns, 900–2500 μm^2	Diagonally-oriented F-actin stress fibers on square patterns, preferential protrusions from corners, ROCK/myosin dependent	[68]
Topography	Rat aortic EC	Titanium grooves, ~150–300nm height, 750nm to 100μm spacing	Greater alignment and elongation and reduced time to confluency with decreased periodicity	[70]
Topography	Endothelial progenitor cell	Parallel grooves and ridges, 600 nm-width	Reduced proliferation and enhanced directional migration compared to flat substrates, enhanced capillary tube formation	[71]
Topography	Primary human dermal microvascular EC	Aligned or randomly oriented collagen fibrils	Distinct focal adhesion organization, greater alignment, and quicker migration along fiber direction for aligned collagen	[72]
Topography	Human umbilical vein EC	Aligned electrospun hyaluronic acid-based fibers	Fiber orientation dominated over chemical VEGF gradient for instruction of cell migration	[73]
Topography and shear flow	Primary human dermal EC	Aligned nanofibrillar collagen and spatially varying flow up to 2.5 Pa	Elongation and migration along fibers even when orthogonal to flow direction, reduced monocyte adhesion and ICAM-1 expression, reduced turnover, enhanced CD31 thickness and continuity	[74]
Substrate stiffness	Human umbilical vein EC	1.72 to 21.5 kPa polyacrylamide (PA) gels	Soft gels: rounded cells, peripheral actin Stiffer gels: spread and spindle-like cells, increased proliferation, more F-actin stress fibers, higher RhoA activity and activation of 3 integrins	[85]
Substrate stiffness	Primary porcine EC	4, 14, and 50 kPa PA gels	Soft gels: highest junction integrity Stiff gels: furthest migration, alignment of deposited ECM	[86]
Substrate stiffness	Human umbilical vein EC	1.2 to 90 kPa PA gels	Increased baseline contractility on stiffer gels; increased gap formation and ROCK activity with thrombin especially on stiffer gels	[89]
Substrate stiffness	Bovine aortic EC	3.5 to 10 kPa PA gels	Increased permeability to dextran dye with increased stiffness	[81]

Mechanical Stimulus	Cell Type	Stimulus Parameters	Results	Reference
Substrate stiffness	Human pulmonary aortic EC	1.1 and 40 kPA PA gels, glass	Greater increases in cell stiffness with VE-cadherin activation by magnetic twisting on softer gels; increased focal adhesion formation with bead twisting, monolayer stress, and susceptibility to gap formation on stiffer substrates	[53]
Substrate stiffness	Human umbilical vein EC	0.42 to 280 kPA PA gels	Greater fraction of transmigrating neutrophils on stiffer gels with TNF-α stimulation, reduced transmigration with contractility inhibition	[90]
Substrate stiffness	Bovine aortic EC	Heterogenous hyaluronic acid-based gels, checkerboard pattern of 2.2 and 10.3 kPa regions	Large focal adhesions on stiff regions; larger and more frequent gaps in VE-cadherin junctions with increased heterogeneity	[92]
Substrate stiffness	Bovine aortic EC	1.7 and 9 kPa 2D PA gels; 125 and 500 Pa 3D collagen gels	Greater cell stiffness on top of and embedded within stiffer gels	[160]
Substrate stiffness	Human blood outgrowth EC and Human umbilical vein EC	Floating and constrained 3D collagen gels	Optimal ratio of effective gel stiffness and contractility supported enhanced capillary morphogenesis	[161]
Substrate stiffness	Human umbilical vein EC co-culture with human mesenchymal stem cell	3D collagen/fibrin gels	Decreased vessel formation with increased stiffness	[162]
Substrate stiffness and shear flow	Bovine aortic EC	100 Pa and 10 kPa PA gels; 0.6 to 2.2 Pa shear	Higher shear required for alignment with flow on softer gels; greater impact of shear on cell spreading on softer gels; spreading blocked by hyaluronan disruption	[93]

Table 2.

Active mechanical stimuli experienced by endothelial cells (ECs) under hemodynamic conditions modulate cell behavior and function

Mechanical Stimulus	Cell Type	Stimulus Parameters	Results	Reference
Shear flow	Bovine aortic EC	1.52 Pa, unidirectional, laminar	Elongation and orientation along flow direction, stress fiber formation	[58]
Shear flow	Bovine aortic EC	2 Pa, unidirectional or alternating directions with 30min interval	Cytoskeletal reorganization precedes alignment, periodically alternating flow reduces alignment	[56]
Shear flow	Bovine aortic EC	Turbulent, 0.15 Pa check	Cell rounding, DNA synthesis, monolayer gap formation	[60]
Shear flow	Human umbilical vein EC	Disturbed flow in step channel: stress fluctuations and high shear gradients	Cell rounding, DNA synthesis	[61]
Shear flow	Bovine aortic EC	Oscillatory flow, 1Hz, 0.05 ± 0.4 Pa	Intermittent VE-cadherin along cell junctions	[62]
Shear flow	Human umbilical vein EC	Unidirectional, laminar, 0.72 Pa	Nucleus pushed downstream, cells polarized against flow	[64]
Stretch	Bovine capillary EC	Static 15% strain	Calcium influx within 5 seconds of stretch, SA channel activation of PI3K and 1 integrins leading to reorganization	[102]
Stretch	Bovine aortic EC	7 and 24% cyclic stretch, 1Hz	Phosphorylation and redistribution of focal adhesion kinase and vinculin with strain leading to alignment perpendicular to stretch	[101]
Stretch	Human aortic EC	10% cyclic stretch	Alignment along direction of minimal substrate deformation (i.e. perpendicular to uniaxial stretch or 70 degrees from direction of simple elongation)	[99]
Stretch	Bovine aortic EC	6–10 and 20% cyclic stretch, 1 Hz	Increased TNF-α-mediated cell death for 20% strain	[100]
Stretch	Human umbilical vein EC	10 and 20% cyclic stretch, 1 Hz	Increased TNF-α production with stretch, increased MMP-2 and MMP-14 levels with 20% stretch	[95]
Stretch	Human umbilical vein EC	7% cyclic stretch	Enhanced directional migration, sprout formation, and production of angiogenic factors	[163]